

Nosetto Marcelo (Orcid ID: 0000-0002-9428-490X)

**Title: Contrasting CO<sub>2</sub> and water vapor fluxes in dry forest and pasture sites of central Argentina**

Nosetto MD<sup>1,2</sup>, Luna Toledo E<sup>3,4</sup>, Magliano PN<sup>1,5</sup>, Figuerola P<sup>4</sup>, Blanco L<sup>3</sup>, Jobbágy EG<sup>1</sup>.

<sup>1</sup> Grupo de Estudios Ambientales, Instituto de Matemática Aplicada San Luis, IMASL, CONICET & Universidad Nacional de San Luis. Ejército de los Andes 950. D5700HHW San Luis, Argentina.

<sup>2</sup> Cátedra de Climatología Agrícola (FCA-UNER), Ruta 11, km 10, Oro verde, Entre Ríos, Argentina

<sup>3</sup> Estación Experimental La Rioja, Instituto Nacional de Tecnología Agropecuaria (INTA), La Rioja, Argentina.

<sup>4</sup> Instituto de Ambiente de Montaña y Regiones Áridas (IAMRA), Universidad Nacional de Chilecito, La Rioja, Argentina.

<sup>5</sup> Departamento de Biología, Facultad de Química, Bioquímica y Farmacia, Universidad Nacional de San Luis, Ejército de los Andes 950. D5700HHW San Luis, Argentina.

Short title: **CO<sub>2</sub> and water vapor fluxes in a dry forest and a pasture of Argentina**

**Abstract**

The dry forests of South America are a key player of the global carbon cycle and the regional water cycle but they are being intensively deforested. We used eddy covariance measurements to compare the temporal patterns of CO<sub>2</sub> and water vapor fluxes and their relationships with environmental variables in dry forest and pastures sites of central Argentina. Ecosystem fluxes showed clear contrasts in magnitude, timing, and response to environmental controls between ecosystems. The dry forest displayed higher daily gross primary productivity (GPP, 10.6 vs. 7.8 g CO<sub>2</sub> m<sup>-2</sup> d<sup>-1</sup>) and ecosystem respiration (R<sub>eco</sub>, 9.1 vs. 7 g CO<sub>2</sub> m<sup>-2</sup> d<sup>-1</sup>) and lower net ecosystem exchange (NEE, -1.5 vs. -0.7 g CO<sub>2</sub> m<sup>-2</sup> d<sup>-1</sup>) than the pasture. These differences were explained by a lower tolerance of the pasture to cool temperatures and drought. The lowest NEE rates were observed between 26 and 34 °C in the pasture but below this range NEE increased sharply, switching to a carbon source with temperatures < 20 °C. By contrast, the dry forest remained as a strong carbon sink down to 18 °C. The pasture also showed a stronger drop of GPP with drought compared to the dry forest, becoming a carbon source with soil wetness < 25% of soil available water. Rainfall was strongly coupled with GPP in both ecosystems but the dry forest responded to longer rainfall integration periods. This study helps to understand how ecosystems can respond to climate change, improve global scale modelling and increase the productivity and resilience of rangelands.

Keywords: eddy covariance; Bowen ratio; net ecosystem exchange; *Cenchrus ciliaris*; NDVI

This article has been accepted for publication and undergone full peer review but has not been through the copyediting, typesetting, pagination and proofreading process which may lead to differences between this version and the Version of Record. Please cite this article as doi: 10.1002/eco.2244

## 1. Introduction

Arid and semi-arid ecosystems (hereafter drylands) cover 45% of Earth's land surface (Právělie, 2016; Schimel, 2010). Despite showing a relatively low mean annual primary productivity, they are a key player of the global carbon cycle (Huston & Wolverton, 2009; Jung et al., 2011). Global scale studies show that while the mean carbon sink is dominated by highly productive regions, drylands drive the inter-annual variability and trend of carbon sinks over recent decades (Ahlström et al., 2015; Jung et al., 2011; Poulter et al., 2014). Moreover, this influence is mostly mediated by changes in gross primary productivity (Ahlström et al., 2015; Jung et al., 2011) which means that the growth of vegetation in drylands is the most important factor governing the global inter-annual variability and trend of carbon sinks. In this context, it is important to highlight that dryland ecosystems are subject to high transformation pressures from the, often interactive, effects of agricultural use and climatic change (Reynolds et al., 2007; Wang et al., 2012).

Understanding the patterns and drivers of CO<sub>2</sub> and water vapor fluxes of ecosystems becomes relevant in a global change context, for instance, to predict expected feedbacks or to improve models relating carbon fluxes to environmental variables. However, most studies have been biased towards more humid systems, whereas studies in (semi)arid ecosystems are not that widespread (Baldocchi, Chu, & Reichstein, 2018; Chen et al., 2015). While most of our current understanding of the patterns and drivers of ecosystem fluxes in drylands has been based on remote sensing studies, coarse-scale atmospheric inversion models, empirical regression models, or terrestrial biosphere models, they are still poorly constrained by field measurements (Biederman et al., 2017). The eddy covariance technique allows for quasi-continuous measurements of whole-ecosystem fluxes of CO<sub>2</sub>, water vapor and energy, offering a valuable approach to fill this gap (Baldocchi, 2003; Law et al., 2002). The use of this technique in South American drylands is more recent but the few existing studies (e.g. García et al., 2017; Silva et al., 2017) have provided key findings on the functioning of these ecosystems.

In drylands, water availability has been identified as a key control of CO<sub>2</sub> fluxes in both native and cultivated ecosystems (Biederman et al., 2016; Newman et al., 2006). For instance, droughts generally lead to a higher drop in gross primary productivity than in ecosystem respiration (Atkin & Macherel, 2009; Schwalm et al., 2010), and consequently, switch ecosystems from carbon sinks to sources (Biederman et al., 2017; Ciais et al., 2005; Scott, Biederman, Hamerlynck, & Barron-Gafford, 2015). Beyond these broad patterns, the finely tune response of ecosystem to fluctuating water inputs is ultimately dependent on their species composition and their adaptations to cope with water shortages (García et al., 2017; Reynolds, Kemp, Ogle, & Fernández, 2004). Given the ongoing climatic change, where a higher frequency of extreme climatic events (more intense rainfalls and longer droughts) are expected for the dry forests of southern South America (Barros et al., 2015; Labraga & Villalba, 2009), a better understanding of the relationship between CO<sub>2</sub> fluxes and water availability is warranted.

The response of CO<sub>2</sub> fluxes to air temperature variability is a critical aspect of ecosystems functioning, particularly in a global warming context. This is crucial, for instance, to understand whether temperature feedbacks on the carbon balance can speed up (or not) the process of global warming (Zeng, Qian, Munoz, & Iacono, 2004). In mesic ecosystems, where rainfall is not the main limiting factor to vegetation growth, temperature increases usually translate into higher ecosystem productivity (Law et al., 2002) and stronger carbon sink (Yi et al., 2010). In drylands, instead, a negative linear relationship between mean annual temperature and vegetation productivity has been observed, both spatially (among sites) and temporally (among years) (Biederman et al., 2017). This would imply that global warming can be accelerated by the aforementioned sink-to-source switches in drylands (Anderson-Teixeira, Delong, Fox, Brese, & Litvak, 2011). Understanding the effects of temperature on CO<sub>2</sub> fluxes of native and cultivated ecosystems in semi-arid regions of South America is important to assess the role of these ecosystems in current and future potential impacts on source-sink dynamics, particularly since this ecosystem type strongly impacts the interannual dynamics of global carbon sinks.

The dry forests of Chaco and Espinal, in southern South America, expand over 1.4 million km<sup>2</sup> and they are the second biggest forest in the continent after Amazonia. This region is one of the few dry forests in the world that still has a large fraction of its natural vegetation (Houspanossian, Giménez, Baldi, & Noretto, 2016). However, deforestation rates have accelerated dramatically in recent decades reaching top records globally (Hansen et al., 2013). The implementation of perennial pastures for cattle grazing, mainly based on African C4 grasses, is the main fate of deforested land in the drier zones of these forests (Houspanossian et al., 2016). Taking into account the potential area of expansion of this transformation, it becomes crucial to understand how land-use changes from forest to pasture affects CO<sub>2</sub> and water vapor fluxes, which in turn influence national and global C inventories, regional atmospheric circulation and subsurface hydrology, among other critical biophysical processes. In addition, given that dry forest and planted pasture differ both functionally and structurally (e.g. C4 vs. C3 species, mono- vs. multi-species composition, deep-rooted vs. shallow-rooted plants), this transformation offers a valuable large scale experiment to analyze how the relevance and strength of environmental drivers on ecosystem fluxes shift with vegetation types.

The main goals of this work were to compare the temporal patterns (weekly, daily and hourly) of CO<sub>2</sub> and water vapor fluxes and to analyze their relationships with air temperature, soil wetness and rainfall under two typical alternative vegetation covers of drylands in central Argentina: native dry forests and planted pastures of the African grass *Cenchrus ciliaris*. For these purposes, we carried out quasi-continuous measurements of these fluxes using the eddy covariance technique in two representative sites of the region during two growing seasons in the case of the dry forest and one growing season in the case of the pasture.

## 2. Materials and methods

### 2.1. Region and study sites

The study area is located in the central part of the dry forests region corresponding to the Dry Chaco phytogeographical province (Fig. 1, Cabrera, 1976). The region is dominated by a forest matrix with some patches of pastures, roller-chopped stands, and grain annual crops (mostly soybean and maize) (Marchesini, Fernández, & Jobbágy, 2013; Steinaker et al., 2016). Extensive cattle raising is the dominant economic activity in the region (Magliano et al., 2019a). The replacement of dry forests by cultivated pastures is the most common strategy of farmers to enhance animal production (Blanco et al., 2005; Kunst et al., 2012). Most pastures are based on C4 grasses such as *Cenchrus ciliaris*, *Panicum maximum* and *Eragrostis curvula*. The stocking rate increases significantly from 0.05 calving units per hectare in native forests to 0.3 in pastures (Karlín, Karlín, Coirini, Reati, & Zapata, 2013). Given that livestock activity may continue to intensify in the future in the region, it is also very likely that this land-use transformation will also increase (Paruelo, Guerschman, Baldi, & Di Bella, 2004). Firewood extraction is restricted to homesteads and it is unusual in the study site (Rueda, Baldi, Gasparri, & Jobbágy, 2015).

The dry forest and pasture sites were 300 km apart in a north-south direction (Fig. 1). The mean annual rainfall in the dry forest site (33.46 S; 66.46 W) is 492 mm y<sup>-1</sup> and Penman-Monteith-FAO reference evapotranspiration approaches 1450 mm y<sup>-1</sup>, what yields a climatic water balance of -958 mm y<sup>-1</sup>. The mean annual temperature is 18 °C and for the coldest (July) and warmest (January) months the mean monthly temperatures are 10.3 °C and 25.4 °C, respectively (1960-1990, Climatic Research Unit, New, Lister, Hulme, & Makin, 2002). The mean annual rainfall and reference evapotranspiration in the pasture site (30.51 S; 66.10 W) are 453 mm y<sup>-1</sup> and 1423 mm y<sup>-1</sup> respectively, which results in a water balance of -970 mm y<sup>-1</sup>. The mean annual temperature is 20.3 °C. The mean temperatures for the coldest (July) and warmest (January) months are 12.5 °C and 27.1 °C, respectively. In both sites, rainfall occurs mostly in late spring and summer (~75% between November and March). (1960-1990, Climatic Research Unit, New et al., 2002). Soils in the study region are derived from fine loessic sediments deposited through the Holocene with some alluvial reworking (Iriando, 1993). Topography is gentle and slopes are <1.5%. Dominant soils are Typic

Torriorthents, well-drained, with 15% clay, 53% sand, and a low organic matter content in the top soil layer (Peña Zubiarte, Anderson, Demmi, Saenz, & D'Hiriart, 1998; Zuzek, 1978).

The dry forest site has a plant composition typical of the native vegetation of the Dry Chaco (Magliano et al., 2016). *Aspidosperma quebracho-blanco* and *Prosopis flexuosa* are the dominant tree species. The understory is dominated by shrub (e.g. *Senna aphylla*, *Moya spinose*, *Larrea divaricata*) and grasses species (e.g. *Stipa eriostachya*, *Aristida mendocina*). The relative canopy covers of trees and shrubs are 82% and 51%, respectively. *Aspidosperma quebracho-blanco* is the tallest tree (12 m), followed by *Prosopis flexuosa* (9 m). The average canopy height in the dry forest approaches 6 m. The pasture site was a former dry forest that was cleared in 1991 to establish a pasture of buffel grass (*Cenchrus ciliaris* L. cv. Texas 4464). After pasture establishment, maintenance practices were performed periodically to avoid woody encroachment. The average canopy height in the pasture during the study period approached 0.30 m. The site was managed with rotational grazing with Aberdeen Angus cattle with a stocking rate of ~0.3 calving unit per hectare. The surface cover by buffel grass approached 85%.

Buffel grass is a C4 perennial bunchgrass, native to subtropical and tropical arid regions of western Asia and Africa (Marshall, Lewis, & Ostendorf, 2012). It is widely distributed in many arid and semi-arid regions of the world as it adapts to a wide range of climates and soils and because it is tolerant to heavy grazing and drought (Marshall et al., 2012). In the study region, buffel grass has a summer growth, beginning to regrow with the first rains of spring (Sep-Oct) and senescing in autumn with the first frosts (Jun-Jul) (Namur, Tessi, Avila, Rettore, & Ferrando, 2014). Its primary productivity is highly dependent on rainfall occurring during the growing season, presenting a forage production rate of 8-10 kg mm<sup>-1</sup> ha<sup>-1</sup> (Avila, Ferrando, Molina, Escribano, & Leal, 2011; Ferrando, Namur, Blanco, Berone, & Vera, 2005).

## 2.2. Environmental and eddy covariance measurements

Environmental and eddy covariance measurements were performed in the centre of paddocks of 1420 ha and 100 ha for the dry forest and pasture, respectively. Net radiation (NR) was measured above the vegetation canopy with net radiometers (NR-Lite, Kipp & Zonen, Delft, The Netherlands). Heat flux was estimated at 5 cm depth (G) with soil heat flux plates (HFP01, Campbell Scientific, Logan, UT, USA) installed under the ground surface in representative locations. Heat storage between the soil surface and the level of eddy covariance measurements was not considered, since its importance is expected to be low in sites with low biomass and short canopies as the ones we studied (Wilson et al., 2002). All additional sources and sinks of energy were considered negligible (Wilson et al., 2002).

Precipitation was measured with tipping-bucket gauges (TE525, Campbell Scientific, Logan, UT, USA) mounted in the measurement towers. Soil volumetric water content was measured with FDR type sensors (ECH<sub>2</sub>O probes, Decagon Devices, Pullman, WA, USA). Sensors were installed at 5, 10, 20 and 50 cm of depth in the dry forest, while in the pasture they were installed only at 10 cm of depth. Given the low precipitation amount that characterizes (semi)arid regions, deep soil layers are more hardly reached by rainfall events, so shallower layers show the greatest temporal variability of soil wetness (Castellanos, Celaya-Michel, Rodríguez, & Wilcox, 2016; Marchesini et al., 2013). Also, it has been observed that soil wetness in surface layers is closely correlated with soil wetness of deeper horizons ( $r^2 = 0.90$ , for soil wetness at 10 cm vs. 50 cm depth;  $p < 0.0001$ , from Marchesini et al., 2013). In addition, surface soil layers usually show the highest concentration of plant roots, particularly in grasslands (Jackson et al., 1996). For all this, soil wetness at 10-cm depth in the pasture is a reasonable indicator of soil available water for vegetation. In the case of the dry forest, we calculated the average soil wetness (0-50 cm depth) by weighting by the thickness of each soil layer.

To homogenize soil wetness measurements in both sites, we calculated the percentage of available water for vegetation based on measurements of water contents at field capacity and permanent wilting point. This relative water content has been proved to be a successful indicator of soil drought

(Reichstein et al., 2002). The water contents at field capacity and wilting point were determined in an empirical way. Field capacity was defined by analyzing soil wetness values 24 hours after precipitation events and permanent wilting point was defined considering the minimum soil wetness registered after more than 2 months with no rainfall. We did not use the standard agronomic permanent wilting point of -1.5 MPa because it is expected that plant species adapted to drought conditions tolerate much more negative water potentials (Chaieb, Floret, Floc'h, & Pontanier, 1992; Marchesini et al., 2013). This approach uses the “plant extraction limit” concept (Seyfried & Wilcox, 2006) and it is assumed that this point coincides well with the lowest soil wetness reading (Castellanos et al., 2016).

Sonic anemometers (CSAT-3, Campbell Scientific, Logan, UT, USA) and open-path infrared gas analyzers (LI-7500, LI-COR, Lincoln, NE, USA) were mounted 10 m and 2.5 m above the ground in the dry forest and pasture sites, respectively. Data of the three components of wind velocity vectors ( $u$ ,  $v$  and  $w$ ), the sonic temperature, and the CO<sub>2</sub> and water vapor air concentrations were sampled at 20 Hz, controlled by Campbell Scientific data loggers (Campbell Scientific, Logan, UT, USA). Instruments were calibrated during the study period and maintenance operations were performed following manufacturer's recommendations. We used the EVEDDY software (Posse et al., 2014) to compute half-hourly eddy fluxes as the covariance between air concentrations of CO<sub>2</sub> (or water vapor) and vertical wind velocity ( $w$ ). We rotated the coordinate system by using the planar fit method for sonic anemometer tilt correction (Wilczak, Oncley, & Stage, 2001). We used the Webb-Pearman-Leuning procedure to correct for density fluctuations due to water vapor and temperature (Webb, Pearman, & Leuning, 1980).

We used EVEDDY to process eddy covariance data (Posse et al., 2014) and we followed standard FLUXNET procedures, which include: despiking, filtering,  $u^*$  correction, flux partitioning and gap filling of half-hourly fluxes (Pastorello et al., 2020). We firstly filtered half-hourly data when rainfall occurred or when poor quality data was detected based on a stationary analysis (Foken et al., 2004). Secondly, we removed half-hourly data higher than two standard deviations from the respective 30-minutes mean determined for a 28-days period centered at the day being considered. Fluxes under calm conditions were removed using a threshold for the critical friction velocity ( $u^*$ ) (Reichstein et al., 2005). To determinate the  $u^*$ -threshold, the data set was divided into six temperature classes of equal sample size. For each temperature class, the data set is split into 20 classes of  $u^*$  of equal size. For each  $u^*$  class, the average flux is calculated, as well as the average flux of all the classes above the  $u^*$  class being considered. The threshold was defined as the  $u^*$ -class where the average night-time flux reaches more than 95% of the average flux at the higher  $u^*$ -classes. The threshold  $u^*$  of each temperature class was only accepted if there was no correlation between temperature and  $u^*$ . The final threshold value was calculated by computing the median of the (up to) six  $u^*$  values corresponding to each temperature class ( $u^* = 0.2 \text{ m s}^{-1}$ ). Ecosystem respiration ( $R_{\text{eco}}$ ) was discriminated from the net ecosystem exchange (NEE) by applying a flux partition approach (Reichstein et al., 2002). After that, we estimated the gross primary productivity (GPP) as the difference between  $R_{\text{eco}}$  and NEE. Finally, a gap filling procedure (Reichstein et al., 2005) was implemented in order to estimate CO<sub>2</sub> fluxes at time scales higher than a half-hour. In this procedure, missing values are replaced by the average value estimated under similar meteorological conditions within a time-window of  $\pm 7$  days. Similar meteorological conditions are satisfied if global radiation, air temperature and vapor pressure deficit do not deviate by more than  $50 \text{ W m}^{-2}$ ,  $2.5 \text{ }^\circ\text{C}$ , and  $500 \text{ Pa}$ , respectively. If similar meteorological conditions could not be found within the  $\pm 7$ -days time window, the averaging window was increased to  $\pm 14$  days (Reichstein et al., 2005). We used the standard sign convention for NEE, with positive values indicating net loss of CO<sub>2</sub> to the atmosphere (ecosystem is acting as a net source) and negative values indicating CO<sub>2</sub> uptake by the ecosystem (ecosystem is acting as a net sink).  $R_{\text{eco}}$  and GPP have always positive values.

The performances of both systems were assessed by statistically examining the energy balance closure during the studied period (Wilson et al., 2002). Half-hourly values of sensible heat flux (H) plus latent heat flux (LE) were compared against the available energy ( $NR - G$ ) by performing linear regression analysis. In the pasture site, the coefficient of determination was 0.93 with an intercept of  $24 \text{ W m}^{-2}$

and a slope of 0.6 ( $p < 0.01$ ). In the case of the dry forest, the coefficient of determination during the study period approached 0.76 with an intercept of  $-17 \text{ W m}^{-2}$  and a slope of 1.07 ( $p < 0.01$ ). The daily energy closures, evaluated with the relation between  $H+LE$  and  $NR-G$ , approached 90% and 96% in the pasture and dry forest sites, respectively. These values are similar to those reported for other sites (Wilson et al., 2002) and evidence a good performance of both systems.

### 2.3. Data analysis

In the pasture site, the measurement and analysis periods was four months, from December 2016 to March 2017, which corresponds to most of the pasture growing season. Unfortunately, due to system failure, the study period could not be extended for a longer time. In the dry forest site, the measurement period extended from December 2009 to March 2011. A first analysis of the patterns and drivers of  $\text{CO}_2$  and water vapor fluxes in this site was performed by García et al. (2017). Because the aim of the current study was to compare both systems, we worked with a data subset of this site, so the analysis period in the dry forest corresponded to December 2009 – March 2010, and December 2010 – March 2011.

In order to better describe the study period, we compared it meteorological conditions against long-term data from the nearest meteorological station of each site. At the nearest meteorological station to the pasture site (Chamical Station, 1990-2020, 24 km from the measurement site), the average temperature and precipitation approached  $26.3 \text{ }^\circ\text{C}$  and 307 mm, respectively, during the study period. These values were similar to long-term means ( $26.1 \text{ }^\circ\text{C}$  and 314 mm) and were within the confidence intervals ( $\alpha = 0.05$ ). At the nearest meteorological station to the dry forest site (San Luis Station, 1990-2020, 22 km from the measurement site), the average temperature and precipitation approached  $23.6 \text{ }^\circ\text{C}$  and 453 mm, respectively, during the study period. These values were also similar to long-term means ( $23.3 \text{ }^\circ\text{C}$  and 425 mm) and were within the confidence intervals ( $\alpha = 0.05$ ).

A similar analysis was performed to compare the ecosystem functioning of both sites during the study period against the long-term behavior. For this purpose, we compared the average values of the satellite variables NDVI, EVI, and surface temperature ( $T_s$ ) derived from MODIS sensor with long-term values (2009-2020). The NDVI and EVI are suitable indexes to assess the condition of the ecosystem, given their connection with primary productivity and green biomass (e.g. Goward & Dye, 1987; Sims et al., 2006). Likewise,  $T_s$  is closely associated with the heat exchange of vegetation canopies with the surrounding atmosphere and particularly with evapotranspiration (e.g. Milkovic, Paruelo, & Noretto, 2019; Rotenberg & Yakir, 2010). For NDVI and EVI, we used the MOD13Q1 product and for  $T_s$  we used the MYD11A2 product. Satellite data was downloaded from the Oak Ridge National Laboratory Distributed Active Archive Center (DAAC, 2018). We selected two areas of  $1 \times 1 \text{ km}$  centred at the measurement towers of the pasture and the dry forest. The means of NDVI, EVI and  $T_s$  for the study period approached 0.51, 0.25 and  $34.0 \text{ }^\circ\text{C}$  respectively in the dry forest, which were within the confidence intervals made with the long-term values (0.49 - 0.55 for NDVI, 0.24 - 0.28 for EVI, and  $33.3 - 34.6 \text{ }^\circ\text{C}$  for  $T_s$ ,  $\alpha = 0.05$ ). In the pasture, the means NDVI, EVI and  $T_s$  for the study period approached 0.38, 0.23 and  $37.4 \text{ }^\circ\text{C}$  respectively and were also within long-term confidence intervals (0.36 - 0.44 for NDVI, 0.22 - 0.28 for EVI, and  $35.1 - 38.1 \text{ }^\circ\text{C}$  for  $T_s$ ,  $\alpha = 0.05$ ). This analysis suggests that the behavior of both studied ecosystems during the study period did not depart from their normal long-term behavior. However, we must be cautious when comparing the absolute values of ecosystem fluxes between both sites since study periods did not overlap.

In addition, we performed another satellite analysis in order to determine the spatial representativeness of our two sites respect to other dry forests and pastures of the area. For this purpose, we selected 10 stands ( $1 \times 1 \text{ km}$  in size) covered by dry forests and 6 with pastures along 30-km radius from our two sites (Fig. 1) and we computed the average monthly values of NDVI, EVI and  $T_s$  for the period 2009-2020. We found that our two study sites were representative of the ecosystems of the region based on the fact that NDVI, EVI and  $T_s$  values were into the confidence intervals ( $\alpha < 0.05$ , Fig. 2).

We evaluated the effects of environmental conditions on CO<sub>2</sub> fluxes and hydrological variables at different temporal scales. At the sub-hourly scale (i.e. 30-minute data), we evaluated the influence of air temperature (measured at ~2.2 m and ~3.5 m above pasture and forest canopies, respectively) on NEE, GEP and R<sub>eco</sub>. In order to remove the effect of solar radiation intensity on stomatal opening, only those measurements performed in the time range of 10:00-17:00 hours were considered in this analysis. In addition, in order to exclude stressful conditions for the vegetation, we filtered out those data with high vapor pressure deficit (VPD ≥ 3 MPa) and low soil wetness (available water ≤ 50%). LOWESS curves were adjusted in order to represent the general trend of the data (Chambers, Cleveland, Kleiner, & Tukey, 1983). At the daily scale, we analyzed the influence of soil wetness on NEE, GEP and R<sub>eco</sub>. Linear regression models were fitted between available water (%) and CO<sub>2</sub> fluxes. We also evaluated the influence of soil wetness on daily evapotranspiration (ET), Bowen ratio (BW = Sensible heat flux / latent heat flux) and water use efficiencies (WUE) of the ecosystem, computed as NEE / ET (i.e. WUE<sub>NEE</sub>) and as GPP / ET (WUE<sub>GPP</sub>). Linear and exponential models were fitted and compared with the Akaike's information criteria (Akaike, 1974). At the weekly scale, we calculated the correlation coefficients between GPP (and ET) and rainfall. In order to assess the time period in which rainfall most strongly influences GPP (and ET), a series of analyses was performed using accumulated precipitation over various periods of time. The integration periods ranged from the current analyzed week to the 10 previous weeks, incremented at one-week intervals. Finally, we analyzed the influence of rainfall events on daily fluxes of NEE, GEE and R<sub>eco</sub> and we obtained the general data trend with LOWESS curves (Chambers et al., 1983).

### 3. Results and Discussion

Over the whole study period, the dry forest displayed higher daily gross primary productivity (GPP) and ecosystem respiration (Reco) than the pasture. Hourly fluxes of CO<sub>2</sub> showed similar temporal dynamics in the dry forest and the pasture, although differences in the absolute values were observed. The dry forest started assimilating CO<sub>2</sub> at 7:00 h local time, one hour after sunrise, and reached a maximum value of 7 μmol CO<sub>2</sub> m<sup>-2</sup> s<sup>-1</sup> around noon, coinciding with the highest incidence of solar radiation (Fig. 3a and 3b). While the pasture began its assimilation of CO<sub>2</sub> at 8:00 h local time, it reached a lower maximum rate of 5.5 μmol CO<sub>2</sub> m<sup>-2</sup> s<sup>-1</sup> at an earlier time, after which a slow decline proceeded. Both sites stopped assimilating CO<sub>2</sub> around 20:30 h, coinciding with the sunset (Fig. 3a and 3b). During most of the day, GPP was higher in the dry forest than in the pasture, with differences of ~1.6 μmol CO<sub>2</sub> m<sup>-2</sup> s<sup>-1</sup> (+30%) at noon (Fig. 3a). During the study period GPP was higher in the dry forest, averaging 10.6 g CO<sub>2</sub> m<sup>-2</sup> d<sup>-1</sup> for both growing seasons (10.45 and 10.71 g CO<sub>2</sub> m<sup>-2</sup> d<sup>-1</sup> for first and second growing season, respectively) versus 7.8 g CO<sub>2</sub> m<sup>-2</sup> d<sup>-1</sup> in the pasture. Ecosystem respiration (R<sub>eco</sub>) rates were rather stable throughout the day, varying between 1.8 and 3 μmol CO<sub>2</sub> m<sup>-2</sup> s<sup>-1</sup> in the dry forest and between 1.6 and 2.3 μmol CO<sub>2</sub> m<sup>-2</sup> s<sup>-1</sup> in the pasture (Fig. 3a). During most of the day, R<sub>eco</sub> was also higher in the dry forest than in the pasture, with maximum differences observed between 14:00 and 16:00 h. On average, R<sub>eco</sub> approached 9.1 g CO<sub>2</sub> m<sup>-2</sup> d<sup>-1</sup> in the dry forest (8.9 and 9.3 g CO<sub>2</sub> m<sup>-2</sup> d<sup>-1</sup> for first and second growing season, respectively) and 7.0 g CO<sub>2</sub> m<sup>-2</sup> d<sup>-1</sup> in the pasture. During the study period both sites behaved as net carbon sinks (Fig. 3c). The dry forest was a net carbon sink (negative NEE values) between 8:00 h and 18:30 h, reaching the minimum rate of -4.3 μmol CO<sub>2</sub> m<sup>-2</sup> s<sup>-1</sup> at noon. The pasture was a net carbon sink between 8:30 h and 19:00 h, and reached the minimum rate of -3.4 μmol CO<sub>2</sub> m<sup>-2</sup> s<sup>-1</sup> before noon. On average for the study period, the daily NEE of the dry forest more than doubled the NEE of the pasture (-1.50 vs. -0.70 g CO<sub>2</sub> m<sup>-2</sup> d<sup>-1</sup>).

The daily minimum NEE rate is a key ecosystem parameter, similar to the maximum photosynthesis rate at the leaf level (Buchmann & Schulze, 1999). The minimum rates of NEE of both the dry forest and the pasture observed in this study were in a low position in the wide range of CO<sub>2</sub> uptake by ecosystems worldwide. The mean minimum NEE rates were only lower than boreal grasslands (-1.6 – -2.3 μmol CO<sub>2</sub> m<sup>-2</sup> s<sup>-1</sup>), similar to some mediterranean evergreen forest (~ -6.8 μmol CO<sub>2</sub> m<sup>-2</sup> s<sup>-1</sup>), a shrub ecosystem (-2.9 – -5.9 μmol CO<sub>2</sub> m<sup>-2</sup> s<sup>-1</sup>) and a boreal spruce forest (-6.3 μmol CO<sub>2</sub> m<sup>-2</sup> s<sup>-1</sup>), but higher than temperate evergreen conifers (-9 – -20 μmol CO<sub>2</sub> m<sup>-2</sup> s<sup>-1</sup>), temperate grasslands (-9 – -25

$\mu\text{mol CO}_2 \text{ m}^{-2} \text{ s}^{-1}$ ), and annual crops ( $-20 - -45 \mu\text{mol CO}_2 \text{ m}^{-2} \text{ s}^{-1}$ ), among others (Eamus, Hutley, & O'Grady, 2001; Falge et al., 2002; Fan et al., 1995; Hastings, Oechel, & Muhlia-Melo, 2005). The very low leaf area indexes of the studied ecosystems, as suggested by MODIS imagery ( $0.9$  and  $0.8 \text{ m}^2 \text{ m}^{-2}$ , for the dry forest and pasture, respectively; data not shown; Abraham et al., 2007; DAAC, 2018; Myneni & Park, 2015) might explain the low  $\text{CO}_2$  assimilation capacity recorded in this study (Buchmann & Schulze, 1999; Hinojo-Hinojo et al., 2019).

Air temperature was strongly correlated with hourly  $\text{CO}_2$  fluxes in these warm-temperate ecosystems (Fig. 4). Note that in this analysis only those measurements performed in the time range of 10:00-17:00 hours were considered. In the pasture, the lowest NEE rates (highest carbon gains) were observed between  $26$  and  $34 \text{ }^\circ\text{C}$  ( $-5.5 \mu\text{mol CO}_2 \text{ m}^{-2} \text{ s}^{-1}$ ); below this temperature range NEE increased sharply (lower carbon gains), switching to carbon source with temperatures  $< 20 \text{ }^\circ\text{C}$  (Fig. 4a). In the forest, the lowest NEE rates occurred between  $22$  and  $28 \text{ }^\circ\text{C}$  ( $-4.9 \mu\text{mol CO}_2 \text{ m}^{-2} \text{ s}^{-1}$ ), with temperatures above and below this range leading to slight NEE increases. This different behavior of both ecosystems resulted in NEE being lower in the forest at low temperatures but in the pasture at high temperatures. The effects of air temperature on NEE were mostly mediated by changes in GPP rather than in  $R_{\text{eco}}$  (Fig. 4b). Maximum GPP rates in the pasture were registered between  $26$  and  $34 \text{ }^\circ\text{C}$  ( $8.1 \mu\text{mol CO}_2 \text{ m}^{-2} \text{ s}^{-1}$ ) but it decreased sharply with cooler temperatures reaching nil rates at  $18 \text{ }^\circ\text{C}$ . In the dry forest, maximum GPP rates were observed between  $23$  and  $28 \text{ }^\circ\text{C}$  ( $7.8 \mu\text{mol CO}_2 \text{ m}^{-2} \text{ s}^{-1}$ ); beyond this range, GPP dropped faster with cooler temperatures (Fig. 4b).

The fact that carbon fluxes in the dry forest and the pasture showed contrasting responses to air temperature is likely explained by the origin (native vs. exotic) and photosynthetic pathway (predominantly C3 vs. C4) of both systems (e.g. Hinojo-Hinojo et al., 2019). The pasture, being composed by the C4 African *Cenchrus ciliaris*, showed higher carbon gains at high temperatures than the dry forest, which is mostly composed by native C3 woody species of the genus *Aspidosperma*, *Prosopis* and *Larrea* (Chaves et al., 2016; García et al., 2017). A similar contrasting pattern between a C4 bunchgrass and mesquite forest was observed by Barron-Gafford et al. (2013). Interestingly, GPP fell so strongly with cool temperatures that the pasture became a carbon source with temperatures  $< 20 \text{ }^\circ\text{C}$ . This low tolerance to cool temperatures strongly constrains the length of the growing season of the pasture and therefore its annual productivity, as observed with biomass cutting approaches (Namur et al., 2014). Because of the temperature effect, the establishment of pastures of *Cenchrus ciliaris* cannot extend much further south than the analysis region (Jerry et al., 1988). It is important to note in this regard that the pasture site has a mean annual temperature two degrees higher than that of the dry forest, being  $300 \text{ km}$  northward. In addition, the lack of vegetation activity in the pasture during large part of the year increases soil moisture and the chances of deep drainage to occur (Castellanos et al., 2016; Gimenez, Nosoetto, Mercau, Paez, & Jobbágy, 2016), which is the main cause of increasing ecosystem salinity in the region (Marchesini, Gimenez, Nosoetto, & Jobbágy, 2016). In the dry forest, GPP also dropped with cool temperatures but to a much lesser extent than in the pasture; in fact it has been observed that even in the cold dry winter ( $T = 10.3 \text{ }^\circ\text{C}$ , mean of the coldest month) the studied forest is able to keep a low but stable carbon assimilation rate (García et al., 2017). The large diversity of plants, which may include complementary thermal niches, characterizing the dry forest of the region (Bogino & Bravo, 2014; García et al., 2017) probably explains the buffered response of GPP to cooler temperatures. From the point of view of forage management, this analysis suggests that the association of buffel grass with C3 species, particularly deep-rooted ones, would be beneficial in order to increase primary productivity (e.g. Glatzle, 2008).

As expected for semi-arid regions, rainfall events triggered large fluxes of  $\text{CO}_2$  especially in the pasture site (Fig. 5). After rain events preceded by dry periods, fast increases in  $R_{\text{eco}}$  and GPP were observed and after a few days ( $\sim 2 - 3$ ) the pasture switched from source to sink behavior (Fig. 5a).  $R_{\text{eco}}$  quickly stabilized after rainfall events (at  $\sim 3.3 \text{ g C m}^{-2} \text{ d}^{-1}$ ), remaining stable for several days and declining afterwards. GPP showed a more abrupt response, increased over a longer time period until a maximum rate of  $7 \text{ g C m}^{-2} \text{ d}^{-1}$  was reached, decreasing steeply after that (Fig. 5a). In the dry forest, it was not possible to identify such clear pattern, although a similar trend can be seen (Fig. 5b). After rainfall events,  $R_{\text{eco}}$  tended to stabilize at  $\sim 2.5 \text{ g C m}^{-2} \text{ d}^{-1}$ , showing a more gradual decline than GPP,



which reached slightly lower maxima (5–6 g C m<sup>-2</sup> d<sup>-1</sup>) than the pasture. Excluding periods with dry soil (available water < 50%), days in which both ecosystems behaved as carbon source were mostly associated with cloudy conditions.

Soil wetness strongly affected daily CO<sub>2</sub> fluxes in both ecosystems (Fig. 6). Increases in available water (AW) led to higher CO<sub>2</sub> fluxes (GPP and R<sub>eco</sub>) in the pasture and the dry forest. While in the dry forest variation rates of R<sub>eco</sub> and GPP as a function of AW were similar (slopes of 0.035 and 0.046 g C m<sup>-2</sup> d<sup>-1</sup> per 1% of AW, respectively), in the pasture GPP varied more strongly than R<sub>eco</sub> (slopes of 0.087 and 0.033 g C m<sup>-2</sup> d<sup>-1</sup> per 1% of AW, respectively). The fitted linear model suggested that the pasture becomes a net carbon source with soil wetness below ~25% of total AW and that GPP approaches zero with 10% of AW. In contrast, in the dry forest, the linear model suggested that it becomes carbon neutral only when complete soil drying was achieved, while GPP was always >1.2 g C m<sup>-2</sup> d<sup>-1</sup> in the full range of AW.

Weekly GPP was associated with rainfall occurring in previous weeks in both ecosystems, but clear differences were observed between them (Fig. 7a). In the forest, the correlation was significant with integration periods ranging from two to nine weeks (p < 0.01, n = 28). But in the pasture, significant correlations were only observed when rainfall was integrated over the previous three or four weeks (p < 0.01, n = 14). Longer and shorter rainfall integration periods showed weaker and non-significant correlations. In addition, the linear models adjusted for the period with the highest correlation showed that the slope was higher in the pasture than in the dry forest (p < 0.10, Fig 7b, inset). This pattern suggests that the pasture presents higher weekly GPP than the dry forest with plenty rainfall, while with meager rainfall GPP is higher in the forest.

The relationships between water availability and carbon assimilation evidence differential functioning between both ecosystems (Figs. 6 and 7a). Despite being considered as a drought tolerant species well adapted to semiarid areas (Marshall et al., 2012), buffel grass showed a stronger fall of net carbon assimilation with drought than the native dry forest, which was explained by a faster drop of gross primary productivity than ecosystem respiration. This contrasting behavior is probably due to the fact that some of the dry forest species have deeper root systems (Canadell et al., 1996; Marchesini et al., 2013) than the pasture which would allow them to use deeper water (Jobbágy, Nosoetto, Villagra, & Jackson, 2011) and sustain a certain carbon gain during rainless periods. There are three main mechanisms that favor water storage at greater depth in the studied dry forest, which include (i) runoff-runon water redistribution that concentrates rainfall and favors percolation in a minor fraction of the area (Magliano, Breshears, Fernández, & Jobbágy, 2015; Magliano, Fernández, Florio, Murray, & Jobbágy, 2017b), (ii) large amounts of stemflow generation by some dominant shrubs such as *Larrea divaricata* (Magliano, Whitworth-Hulse, Florio, Aguirre, & Blanco, 2019c) and (iii) the low atmospheric demand at the soil surface level caused by canopy shade and litter that maintains wet soil conditions increasing the probability that the next rain event reaches greater depths (Magliano et al., 2017a). In addition, deep soil layers (> 1 m) under dry forests of the region are typically salty because of long-term accumulation of atmospheric salts resulting from an exhaustive use of rainfall inputs by plants (Santoni, Jobbágy, & Contreras, 2010). This salty condition may constrain water absorption by tree roots, avoiding a complete drying of the soil and lengthening the use of such water source (Marchesini et al., 2013). Likewise, the response of GPP in the pasture to only short periods of rainfall integration (Fig. 7a) suggests a stronger dependence on a small water reservoir, supporting our previous thoughts. Considering an expected climatic scenario of increasing drought episodes (Huntington, 2006; Trenberth et al., 2007), this change of the ecosystem functioning becomes even more relevant given that planted pastures might be more vulnerable and have greater productivity losses under these conditions.

On average and during drought conditions, the dry forest was a stronger carbon sink; however, during periods with high soil wetness the pasture showed the highest net carbon assimilation rates (Fig. 6). For instance, the mean NEE for the first decile (i.e. for the 10% of the days with the lowest NEE values) was almost doubled in the pasture compared to the dry forest (-3.1 vs. -1.7 g C m<sup>-2</sup> d<sup>-1</sup>). Daily NEE rates of the dry forest were similar to other dry ecosystems (Scott, Jenerette, Potts, & Huxman,

2009; Silva et al., 2017; Wohlfahrt, Fenstermaker, & Arnone III, 2008). However, the rates in the pasture during humid periods exceeded them greatly, likely evidencing the higher capacity of CO<sub>2</sub> assimilation of C4 species compared to C3 species (Gowik & Westhoff, 2011; Sage & Zhu, 2011). This contrast between native C3 vegetation and C4 pastures has already been observed in other ecosystems (e.g. Hinojo-Hinojo et al., 2019; Silva et al., 2017) and it is explained by an enhanced primary productivity of the pasture given that when soil was wet (AW > 50%) GPP of the pasture exceeded the dry forest by a quarter, but when soil was dry (AW < 25%) GPP in the dry forest was four-times higher than in the pasture. In other words, the dry forest is more productive than the pasture in the long run as a result of a better performance during (more frequent) dry periods that overcompensates a lower performance during (less frequent) humid periods. However, it is interesting to note that the establishment of pastures in the region allows a notable increase in the carrying capacity of the ecosystem (from ~0.05 to ~0.3 calving unit per hectare), which is probably due to the fact that carbon gains in the pasture are mainly destined to more consumable/palatable plant structures.

Soil wetness not only affected the daily magnitude of ecosystem carbon uptake but also the hourly dynamic in the case of the pasture (Fig. 8). In the dry forest, daily maximum rates of GPP decreased by a third (5.7 vs. 8.4  $\mu\text{mol CO}_2 \text{ m}^{-2} \text{ s}^{-1}$  for periods with AW < 50% and AW > 50%, respectively) during periods with soil water shortage (AW < 50%), but the hourly pattern of GPP did not change (Fig. 8a). In fact, maximum GPP rates were observed in both dry and wet periods close to noon. In the pasture, daily maximum GPP rates decreased more steeply in dry periods than in the forest (-55%, 3.8 vs. 8.6  $\mu\text{mol CO}_2 \text{ m}^{-2} \text{ s}^{-1}$  for periods with AW < 50% and AW > 50%, respectively) and took place earlier in the day (Fig. 8b). With high soil wetness GPP peaked around noon (13:00 – 14:00 h.), while during dry periods the peak occurred in the morning (9:30 – 11:30 h) (Fig. 8b). After this peak, there was a sharp fall of GPP that stabilized around 13:00 h at 2.3  $\mu\text{mol CO}_2 \text{ m}^{-2} \text{ s}^{-1}$  and remained stable until 18:30, decreasing later until sunset.

Hydrological variables were also strongly affected by water availability but different responses were observed in both vegetation covers (Fig. 9). During the study period, evapotranspiration (ET) was ~30% higher in the dry forest compared to the pasture (1.85 vs 1.4  $\text{mm d}^{-1}$ ) and in both systems it was linearly related to soil wetness and rainfall (Fig. 9a and Fig. 7b inset). In the dry forest, weekly ET was significantly correlated with rainfall occurring up to nine previous weeks (Fig. 7b). In the pasture, significant correlations between weekly GPP and rainfall were observed when rainfall was accumulated over shorter periods (2 – 5 weeks,  $p < 0.01$ ,  $n = 14$ , Fig. 7b). The Bowen Ratio (BR), a measure of the partition of surface heat fluxes, showed contrasting behaviors at both sites. As the soil dried, the proportion of heat dissipated in the sensible form increased (higher BR) in both ecosystems but, while in the dry forest it increased linearly, in the pasture it did exponentially (Fig. 9b). In the 5-15% range of AW, only 15% of dissipated heat was in the latent form in the pasture, while in the forest this value averaged 25%. Fitted model suggested that the proportion of heat dissipated in latent and sensible forms was similar (i.e. BR = 1) at 60% of AW in the pasture and at 69% in the dry forest.

Evapotranspiration contrasts between the pasture and the dry forest were mostly observed immediately after rainfall events and also after a few days since the event (Fig. 10). For instance, the ET in the dry forest exceeded the pasture by 30% on average for the three days that followed a rainfall event and by 22% for the period between the ninth and fourteenth days after the rainfall event (Fig. 10). By contrast, no differences were observed during the period between the fourth and eighth day after rainfall. Forests usually show higher ET rates than grasses because they have a better access to deep water sources (i.e. water supply effect) because of deeper roots (Jackson et al., 1996) and/or an enhanced evapotranspiration capacity (i.e. water demand effect) because of higher net radiation, advective energy, or increased evaporating surface (Calder, 1998; Jackson et al., 2008). In our study, we suggest that this last effect was the most important factor driving ET contrasts between the dry forest and the pasture for days immediately after rainfall occurred, because it would have increased interception water loss in the former. It has been observed that interception, which occurs after rainfall events, can be a relevant component of the water balance in (semi)arid regions (Magliano, Whitworth-Hulse, & Baldi, 2019b), particularly in ecosystems with high aerial biomass like the studied dry forest

(Houspanossian, Nosetto, & Jobbágy, 2013). For instance, interception rates of up to four times higher have been measured in dry forests of the region compared to pastures (Magliano et al., 2016). Likewise, the deeper root system would have allowed the dry forest to sustain higher ET rates than the pasture during drought, pattern already observed in grassland areas that were afforested (Milkovic et al., 2019; Nosetto, Jobbágy, Brizuela, & Jackson, 2012).

The water use efficiency (WUE), considering both the net (NEE) and gross (GPP) CO<sub>2</sub> exchange, showed contrasting behavior in both ecosystems (Fig. 9c and 9d). The WUE considered as the ratio NEE / ET (WUE<sub>NEE</sub>) did not show a statistically significant association with the AW in the dry forest but in the pasture (Fig. 9c). In the later, as the soil dried, the WUE<sub>NEE</sub> increased exponentially ( $r^2 = 0.66$ ), which means that less CO<sub>2</sub> was effectively fixed by the ecosystem (or more CO<sub>2</sub> was released; i.e. positive WUE<sub>NEE</sub> values) per liter of water evapotranspired. A similar pattern was observed for WUE<sub>GPP</sub>, with the amount of CO<sub>2</sub> assimilated per liter of water evapotranspired decreasing exponentially ( $r^2 = 0.35$ ) as the soil dried. By contrast in the dry forest, the WUE<sub>GPP</sub> increased linearly as the AW decreased (Fig. 9d).

The WUE is a key variable that links carbon and water cycles. During drought, leaf-level WUE usually increases since partial stomatal closure results in a stronger decrease of transpiration than photosynthesis (Li, Li, Li, & Zhang, 2017; Liu, Andersen, Jacobsen, & Jensen, 2005; Zhang, Jiang, Song, Jin, & Zhang, 2018). However, at the whole ecosystem level, the effect of drought on WUE is more complex as other processes such as soil evaporation or memory effects intervene (Xu, Wang, Zhao, & Zhang, 2019; Yang et al., 2016). In fact, we found contrasting responses between both ecosystems, with the forest showing an increase of WUE during drought and the pasture showing a decrease. Among the processes that could explain this pattern we believe that changes in the energy balance triggered by stomatal closure (Fig. 8b) may be particularly relevant in our study site. During drought, evaporative cooling is reduced and consequently leaf temperature increases (Jones, 1999; Jones et al., 2009), what can trigger different physiological processes (e.g. leaf photodamage, xylem embolism) that reduce carbon gain and therefore WUE (Chaves et al., 2016; Reichstein et al., 2002). We found, for instance, that during drought the surface temperature in the pasture was up to 4.4 °C higher than in neighboring dry forests (34.6 vs. 30.2 °C, based on MOD11A2 Modis imagery, data not shown), which is also evidenced by the sharp increase of the Bowen Ratio (Fig. 9b). By contrast, in the dry forest, the higher capacity of sensible heat dissipation of the canopy (Rotenberg & Yakir, 2010) would prevent surface temperature from raising so much during droughts. Likewise, WUE could also decrease in the pasture during drought because a larger proportion of evapotranspiration would result from abiotic evaporation, especially considering its higher surface temperature.

#### 4. Summary and Conclusions

The dry forests of southern South America are being replaced at rapid rate by exotic grass, raising questions about impacts of this transformation on ecosystem CO<sub>2</sub> and water vapor fluxes. Here, we showed that not only the magnitudes of these ecosystem fluxes, but their timing and sensitivity to water availability and air temperature variation are affected by this land-use change. During the study period, the dry forest had a higher net carbon gain than the pasture, mainly as a result of higher gross primary production rather than lower respiration. This was apparently caused by a lower sensitivity of GPP to drought in forests. This contrast was evident at multiple temporal scales, including daily (noon effect), weekly (post-rainfall response) and seasonal (dry/wet season contrasts, García et al., 2017). A likely explanation for this behavior may be found in a higher soil water storage and a slower soil water release in the dry forests modulated by more preferential downward water fluxes, deeper roots and deep soil salt accumulation (Marchesini et al., 2013). In opposition, pastures had higher gross production rates in wet periods but lower overall rates for this flux. The observed contrast suggests that in rainier years pastures can have higher net carbon gains than forests. However, we should be cautious extrapolating to extreme conditions (e.g. extremely wet or dry periods) given the limitation of the data set. In relation to the effect of air temperature on ecosystem fluxes, we found a lower tolerance of the pasture to cold temperatures, which is in agreement with the general observed failure

of this land use towards the south of the region, suggesting that other pastures species, preferably C3, may yield higher forage production. The dry forest seems to be better adapted to cold temperatures, maintaining a significant CO<sub>2</sub> gain even at the low winter temperatures (García et al., 2017). In the pasture we also found that the water use efficiency decreased as the soil drought increased, an inverse pattern to that commonly observed at the leaf level. The higher values of Bowen ratio and surface temperature observed in the pasture compared to the dry forest during drought periods suggest that thermal stress may be behind the observed patterns. Finally, our study showed that the dynamics of both ecosystems are especially contrasting in their timing and response to extremes more than in their average behavior. This marks important keys to understand (i) how they can respond to climate changes, and (ii) how pastures with more species could be designed in order to show more stable and resilient behaviors.

## **ACKNOWLEDGMENTS**

This work was funded by grants from ANPCyT (Argentina, PICT 2790/14, PICT 4136/16) and CONICET (Argentina, PIP 112-201501-00609). The data that support the findings of this study are available from the corresponding author upon reasonable request. We also thank two anonymous reviewers for their valuable comments to improve the manuscript.

### **Data Availability Statement:**

The data that support the findings of this study are available from the corresponding author upon reasonable request.

**Conflict of Interest:** None.

Accepted

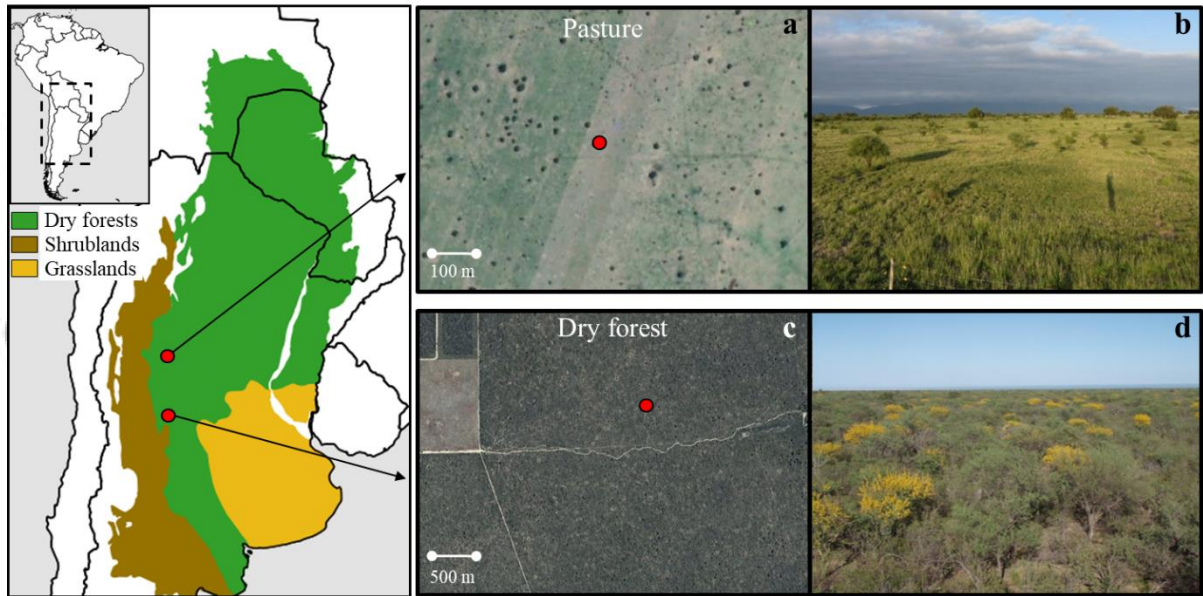


Figure 1. Location of study sites within the dry forest domain of central Argentina. The original extension of the dominant biomes is indicated including the Dry Chaco and Espinal phytogeographical units within the dry forest biome. On the right, Google Earth images (a and c) and photographs (b and d) obtained from the top of the eddy covariance towers (red dots) at each site are shown.

Accepted

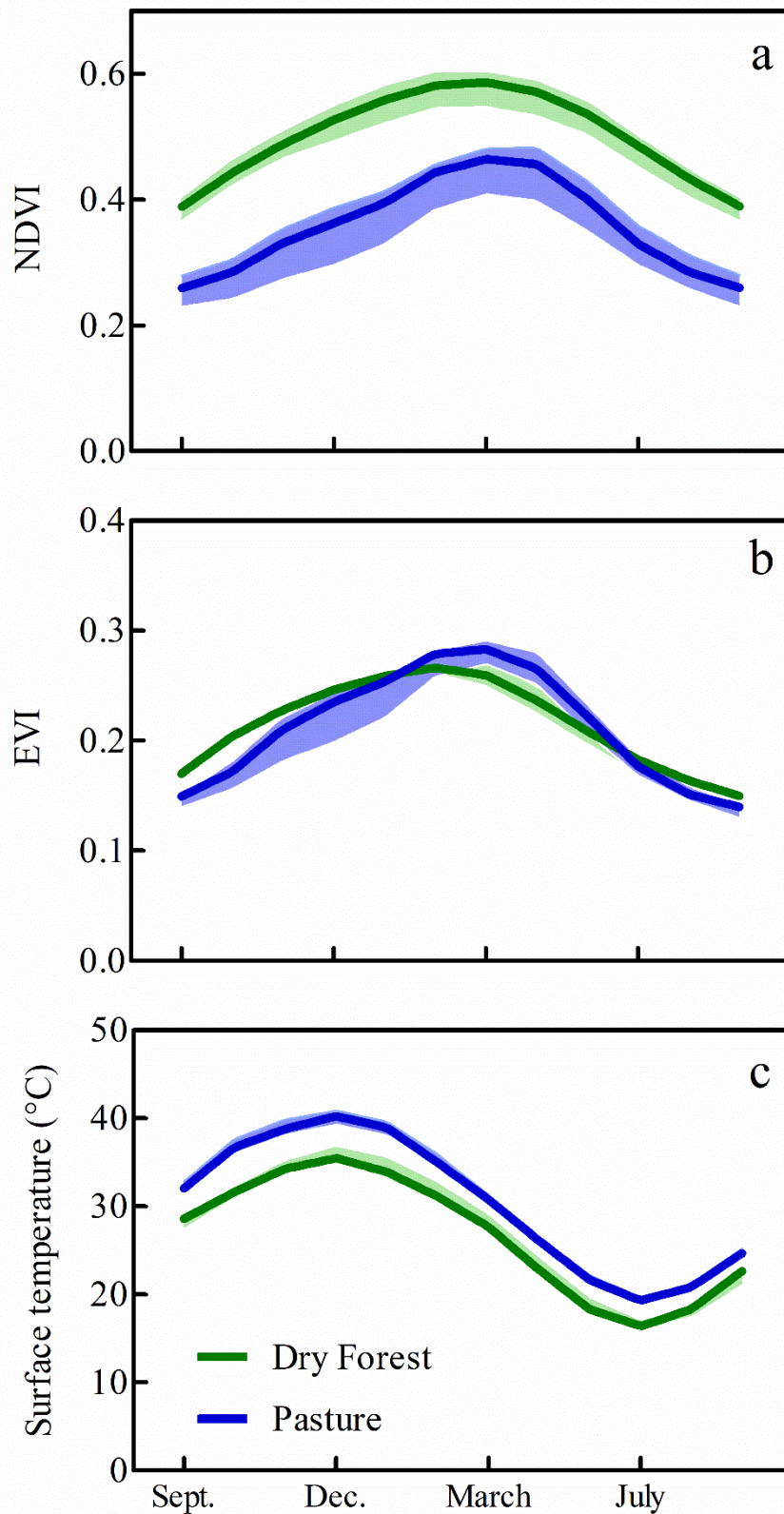


Figure 2. Temporal dynamics of NDVI, EVI and surface temperature in dry forests and pastures. Satellite data was obtained from MODIS imagery. Lines indicate mean monthly values at each study site and shaded areas indicate confidence intervals ( $\alpha = 0.05$ ;  $n = 10$  dry forest stands and 6 pasture stands). The analyzed period was 2009-2020.

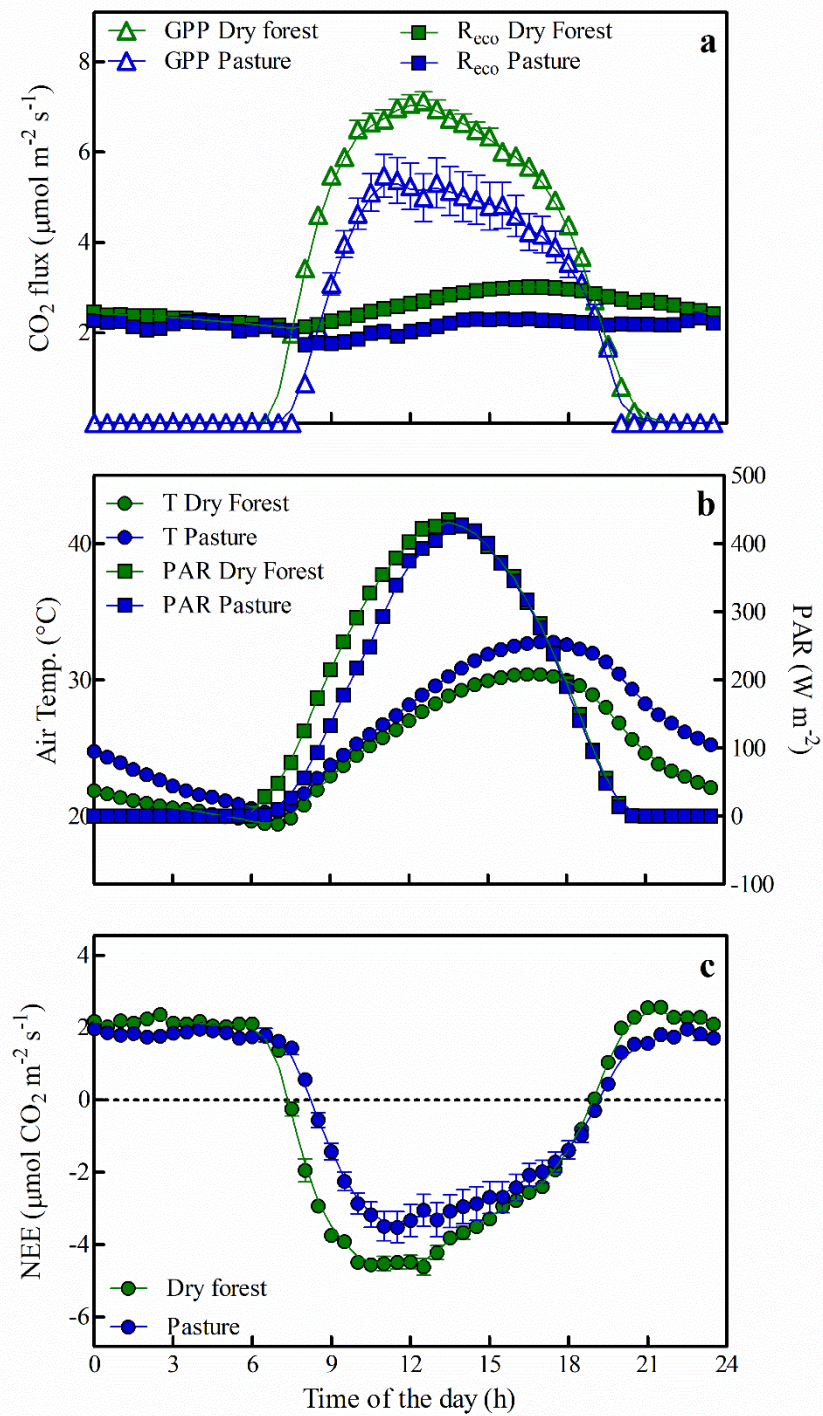


Figure 3. Daily cycles of gross primary productivity (GPP, a), ecosystem respiration ( $R_{\text{eco}}$ , a), photosynthetic active radiation (PAR, b), air temperature (T, b) and net ecosystem exchange (NEE, c). Each dot indicates mean values and vertical lines the standard error for the whole analyzed period. LOWESS curves were fitted to the each dataset.

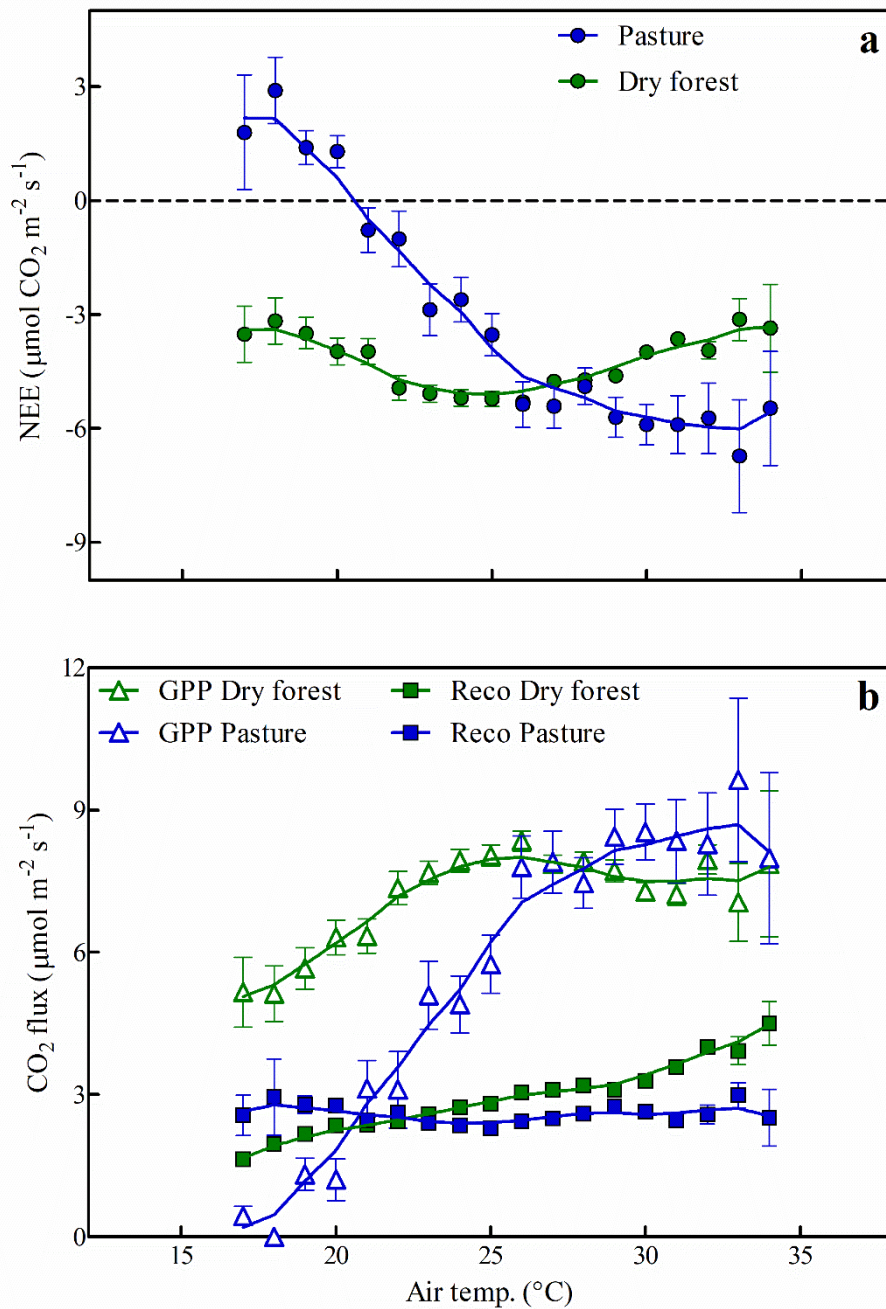


Figure 4. Relationships between net ecosystem exchange (NEE, a), gross primary productivity (GPP, b) and ecosystem respiration ( $R_{\text{eco}}$ , b) with air temperature for the dry forest and pasture sites. Stressful condition for vegetation were filtered out in this analysis ( $\text{VPD} > 3 \text{ kPa}$  and available water  $< 50\%$ ). Each dot indicates mean values and vertical lines indicate the standard error. LOWESS curves were fitted in all cases.



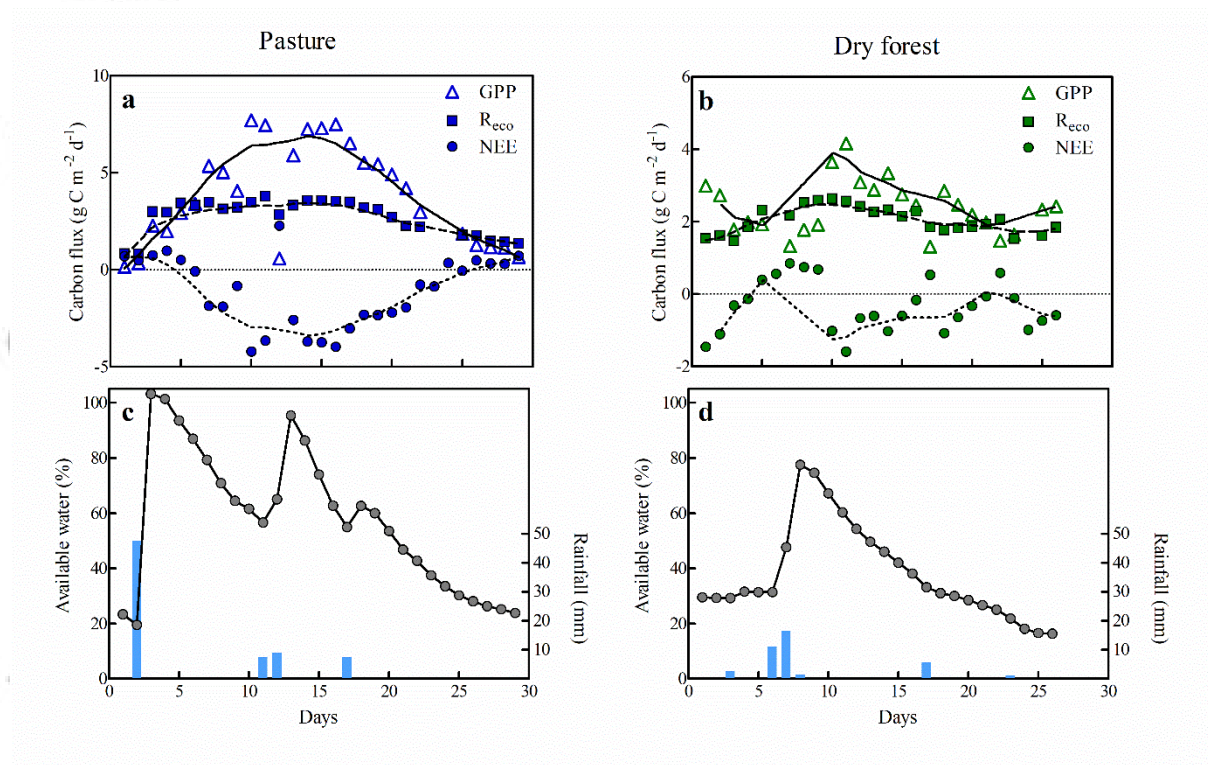


Figure 5. Daily patterns of CO<sub>2</sub> flux and soil available water during and after individual rainfall events at the pasture (a and c – 01/30/2017 – 02/27/2017) and dry forest (b and d – 02/15/2010 – 03/12/2010) sites. The size of rainfall events is indicated in the right y axis. LOWESS curves were fitted to CO<sub>2</sub> fluxes.

Accepted

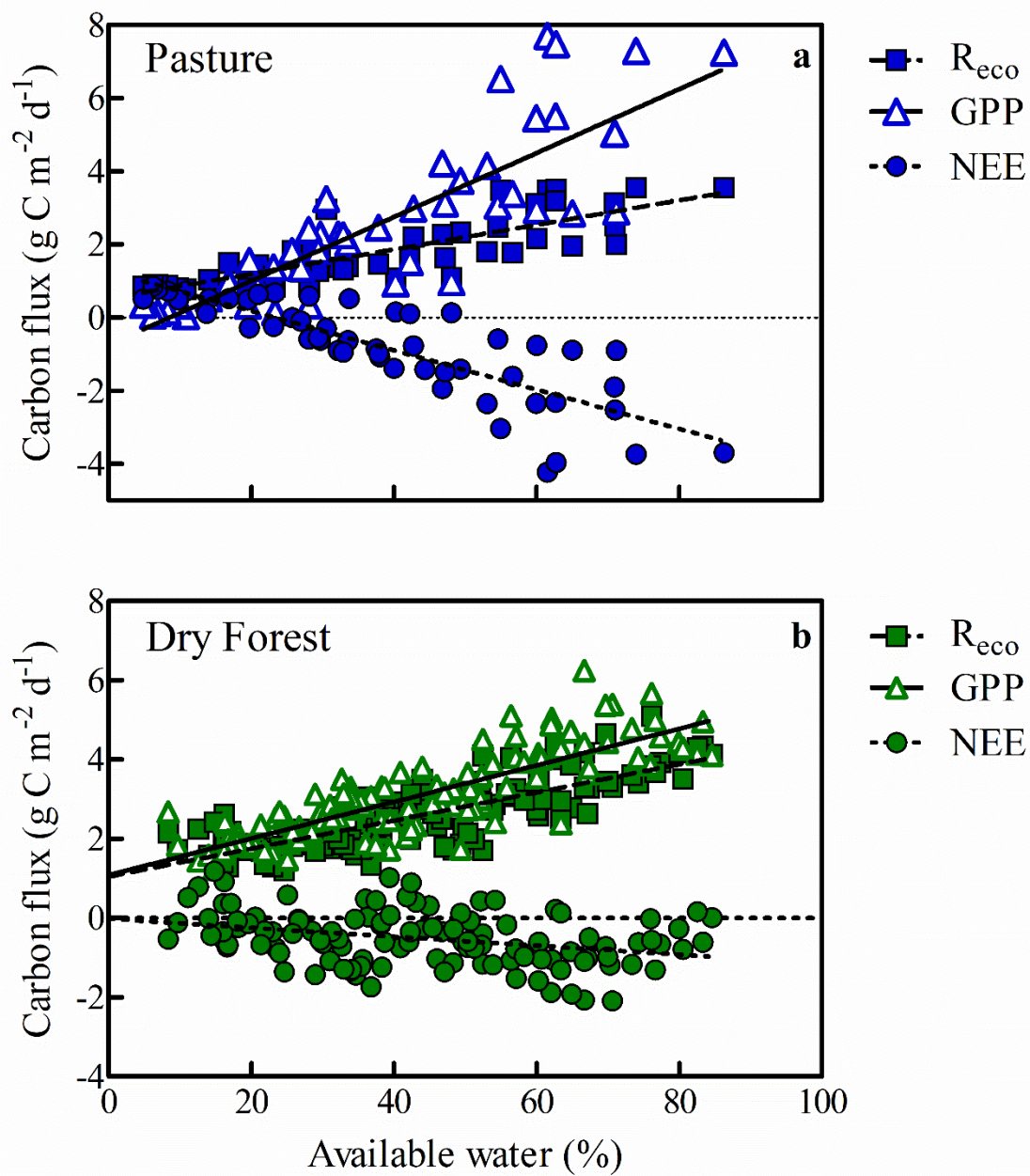


Figure 6. Daily CO<sub>2</sub> fluxes ( $R_{eco}$ , GPP and NEE) as a function of available water in the pasture (a) and dry forest (b) sites. Linear regression models were adjusted in all cases. Soil available water was calculated considering water contents at field capacity (100% of available water) and permanent wilting point (0% of available water) of each site.

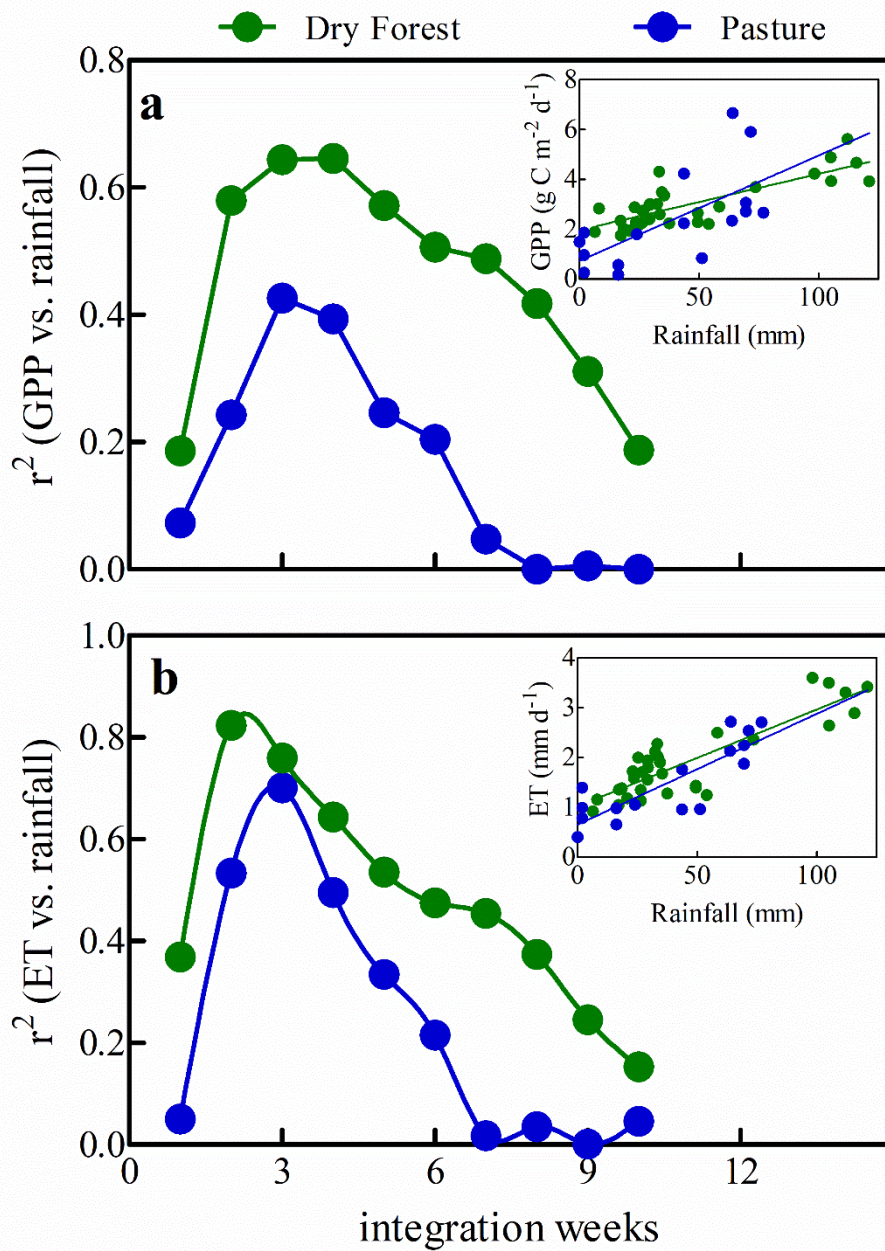


Figure 7. Determination coefficients ( $r^2$ ) between weekly GPP (a) and weekly ET (b) versus rainfall integrated over different time periods. The inset panels showed the relationships between GPP vs. rainfall (a) and ET vs. rainfall (b) for the integration period with the highest determination coefficient.

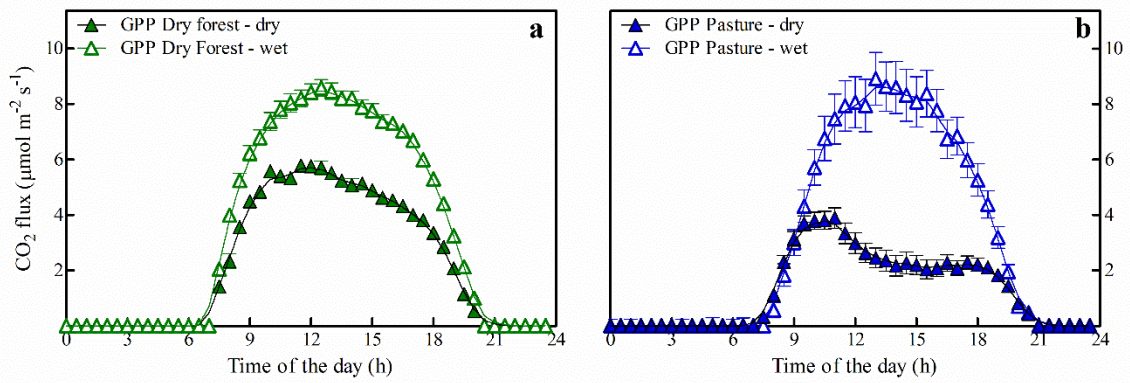


Figure 8. Daily cycles of gross primary productivity (GPP) for the dry forest and pasture sites during periods with dry and wet soil conditions. During the dry period available water was <50 % and during wet periods >50%. Mean values for each period are shown. Vertical lines indicate standard errors. LOWESS curves were fitted in all cases.

Accepted A

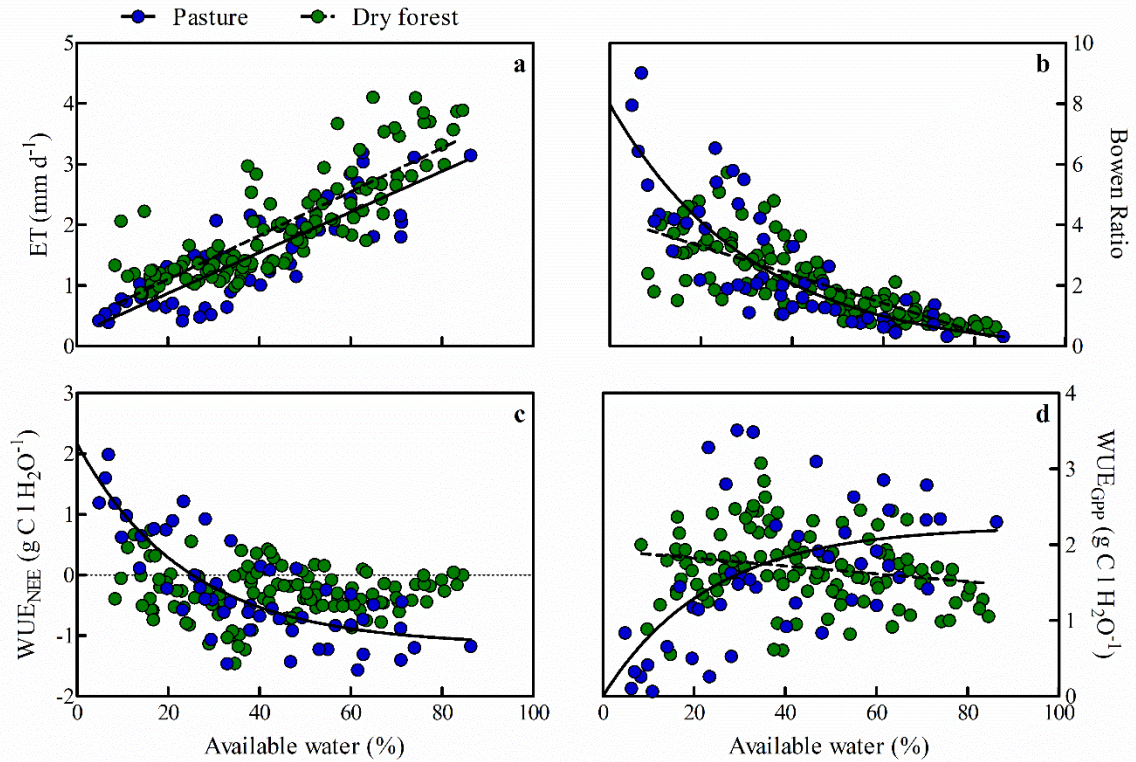


Figure 9. Evapotranspiration (ET, a), Bowen Ratio (b) and Net and Gross Water Use Efficiency ( $\text{EUA}_{\text{NEE}} = \text{NEE} / \text{ET}$ , c and  $\text{EUA}_{\text{GPP}} = \text{GPP} / \text{ET}$ , d) as a function of soil available water at the pasture and dry forest sites. Linear or exponential models were selected based on Akaike's criteria. Soil available water was calculated considering water contents at field capacity (100% of available water) and permanent wilting point (0% of available water) at each site.

Accepted

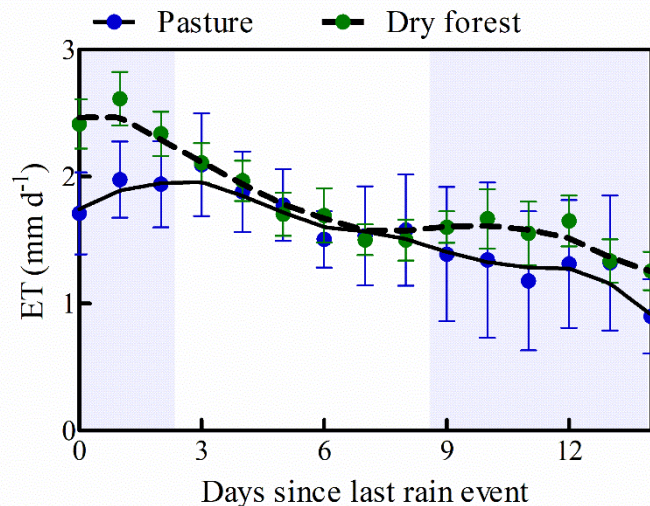


Figure 10. Evapotranspiration rates at successive days following single rainfall events. Each dot corresponds to the mean and standard error of each successive day (0 = day of the rainfall event). Shaded zones indicate successive days in which the dry forest and the pastures displayed significant differences ( $p < 0.05$ ).

## References

- Abraham, E, Abad, J, Lora Borrero, B, Salomón, M, Sánchez, C, & Soria, D. (2007). *Caracterización y valoración hidrológica de la cuenca del Río Mendoza mediante elaboración de modelo conceptual de evaluación*. Paper presented at the XXI Congreso Nacional del Agua, Tucumán, Argentina.
- Ahlström, Anders, Raupach, Michael R., Schurgers, Guy, Smith, Benjamin, Arneeth, Almut, Jung, Martin, . . . Zeng, Ning. (2015). The dominant role of semi-arid ecosystems in the trend and variability of the land CO<sub>2</sub> sink. *Science*, 348(6237), 895. doi: 10.1126/science.aaa1668
- Akaike, H. (1974). A new look at the statistical model identification. *IEEE Transactions on Automatic Control*, 19(6), 716-723.
- Anderson-Teixeira, Kristina , Delong, John , Fox, Andrew , Brese, Daniel , & Litvak, Marcy. (2011). Differential responses of production and respiration to temperature and moisture drive the carbon balance across a climatic gradient in New Mexico. *Global Change Biology*, 17(1), 410-424. doi: 10.1111/j.1365-2486.2010.02269.x
- Atkin, Owen K., & Macherel, David. (2009). The crucial role of plant mitochondria in orchestrating drought tolerance. *Annals of botany*, 103(4), 581-597. doi: 10.1093/aob/mcn094
- Avila, R E, Ferrando, C A, Molina, J P, Escribano, C, & Leal, K. (2011). Acumulación forrajera de *Cenchrus ciliaris* y su relación con las lluvias en La Rioja. *Revista Argentina de Producción Animal*, 31(1), 544.
- Baldocchi, D. (2003). Assessing the eddy covariance technique for evaluating carbon dioxide exchange rates of ecosystems: past, present and future. *Global Change Biology*, 9(4), 479-492. doi: 10.1046/j.1365-2486.2003.00629.x
- Baldocchi, Dennis, Chu, Housen, & Reichstein, Markus. (2018). Inter-annual variability of net and gross ecosystem carbon fluxes: A review. *Agricultural and Forest Meteorology*, 249, 520-533. doi: https://doi.org/10.1016/j.agrformet.2017.05.015
- Barron-Gafford, Greg A., Scott, Russell L., Jenerette, G. Darrel, Hamerlynck, Erik P., & Huxman, Travis E. (2013). Landscape and environmental controls over leaf and ecosystem carbon dioxide fluxes under woody plant expansion. *Journal of Ecology*, 101(6), 1471-1483. doi: 10.1111/1365-2745.12161

- Barros, V. R., Boninsegna, J. A., Camilloni, I. A., Chidiak, M., Magrín, G. O., & Rusticucci, M. (2015). Climate change in Argentina: Trends, projections, impacts and adaptation. *Wiley Interdisciplinary Reviews: Climate Change*, 6(2), 151-169. doi: 10.1002/wcc.316
- Biederman, Joel A., Scott, Russell L., Bell, Tom W., Bowling, David R., Dore, Sabina, Garatuza-Payan, Jaime, . . . Goulden, Michael L. (2017). CO<sub>2</sub> exchange and evapotranspiration across dryland ecosystems of southwestern North America. *Global Change Biology*, 23(10), 4204-4221. doi: 10.1111/gcb.13686
- Biederman, Joel A., Scott, Russell L., Goulden, Michael L., Vargas, Rodrigo, Litvak, Marcy E., Kolb, Thomas E., . . . Burns, Sean P. (2016). Terrestrial carbon balance in a drier world: the effects of water availability in southwestern North America. *Global Change Biology*, 22(5), 1867-1879. doi: 10.1111/gcb.13222
- Blanco, Lisandro J., Ferrando, Carlos A., Biurrun, Fernando N., Oriente, Enrique L., Namur, Pedro, Recalde, Dario J., & Berone, German D. (2005). Vegetation Responses to Roller Chopping and Buffelgrass Seeding in Argentina. *Rangeland Ecology & Management*, 58(3), 219-224. doi: [https://doi.org/10.2111/1551-5028\(2005\)58\[219:VRTRCA\]2.0.CO;2](https://doi.org/10.2111/1551-5028(2005)58[219:VRTRCA]2.0.CO;2)
- Bogino, S., & Bravo, M. (2014). Impacto del rolado sobre la biodiversidad de especies leñosas y la biomasa individual de jarilla (*Larrea divaricata*) en el Chaco Árido Argentino. *Quebracho*, 22, 79-87.
- Buchmann, N., & Schulze, E D. (1999). Net CO<sub>2</sub> and H<sub>2</sub>O fluxes of terrestrial ecosystems. *Global Biogeochemical Cycles*, 13(3), 751-760.
- Cabrera, A L. (1976). *Regiones fitogeográficas argentinas* (Vol. 2). Buenos Aires: ACME.
- Calder, Ian R. (1998). Water use by forests, limits and controls. *Tree Physiology*, 18, 625-631.
- Canadell, J, Jackson, R B, Ehleringer, J R, Mooney, H A, Sala, O E, & Schulze, E D. (1996). Maximum rooting depth of vegetation types at the global scale. *Oecologia*, 108, 583-595.
- Castellanos, Alejandro E., Celaya-Michel, Hernán, Rodríguez, Julio C., & Wilcox, Bradford P. (2016). Ecohydrological changes in semiarid ecosystems transformed from shrubland to buffelgrass savanna. *Ecohydrology*, 9(8), 1663-1674. doi: 10.1002/eco.1756
- Ciais, Ph, Reichstein, M., Viovy, N., Granier, A., Ogée, J., Allard, V., . . . Valentini, R. (2005). Europe-wide reduction in primary productivity caused by the heat and drought in 2003. *Nature*, 437, 529.
- Chaieb, M., Floret, C., Floc'h, E. Le, & Pontanier, R. (1992). Life history strategies and water resource allocation in five pasture species of the Tunisian arid zone. *Arid Soil Research and Rehabilitation*, 6(1), 1-10. doi: 10.1080/15324989209381291
- Chambers, J M, Cleveland, W S, Kleiner, B, & Tukey, P A. (1983). *Graphical methods for data analysis*: Wadsworth and Brooks.
- Chaves, M. M., Costa, J. M., Zarrouk, O., Pinheiro, C., Lopes, C. M., & Pereira, J. S. (2016). Controlling stomatal aperture in semi-arid regions—The dilemma of saving water or being cool? *Plant Science*, 251, 54-64. doi: <https://doi.org/10.1016/j.plantsci.2016.06.015>
- Chen, Zhi, Yu, Guirui, Zhu, Xianjin, Wang, Qiufeng, Niu, Shuli, & Hu, Zhongmin. (2015). Covariation between gross primary production and ecosystem respiration across space and the underlying mechanisms: A global synthesis. *Agricultural and Forest Meteorology*, 203, 180-190. doi: <https://doi.org/10.1016/j.agrformet.2015.01.012>
- DAAC, ORNL. (2018). MODIS and VIIRS Land Products Global Subsetting and Visualization Tool. ORNL DAAC, Oak Ridge, Tennessee, USA. Accessed February 08, 2019. Subset obtained for MOD13Q1 product at 42.2955S,71.1496W, time period: 2000-02-18 to 2019-01-01, and subset size: 0.25 x 0.25 km. <https://doi.org/10.3334/ORNLDAAAC/1379>.
- Eamus, Derek, Hutley, Lindsay B., & O'Grady, Anthony P. (2001). Daily and seasonal patterns of carbon and water fluxes above a north Australian savanna. *Tree Physiology*, 21(12-13), 977-988. doi: 10.1093/treephys/21.12-13.977
- Falge, Eva, Tenhunen, John, Baldocchi, Dennis, Aubinet, Marc, Bakwin, Peter, Berbigier, Paul, . . . Wofsy, Steve. (2002). Phase and amplitude of ecosystem carbon release and uptake potentials as derived from FLUXNET measurements. *Agricultural and Forest Meteorology*, 113(1-4), 75-95. doi: [http://dx.doi.org/10.1016/S0168-1923\(02\)00103-X](http://dx.doi.org/10.1016/S0168-1923(02)00103-X)
- Fan, S M, Goulden, M L, Wunger, J W, Daube, B C, Bakwin, P S, Wofsy, S C, . . . Moore, T R. (1995). Environmental controls on the photosynthesis and respiration of a boreal lichen

- woodland: a growing season of whole-ecosystem exchange measurements by eddy correlation. *Oecologia*, 102(4), 443-452.
- Ferrando, C A, Namur, Pedro, Blanco, Lisandro J, Berone, G, & Vera, T. (2005). Módulo experimental de cría sobre buffel grass – pastizal natural en Los Llanos de La Rioja: Indices productivos. *Revista Argentina de Producción Animal*, 25(1), 316-317.
- Foken, T, Göckede, Mathias, Mauder, M, Mahrt, L, Amiro, B, & W, Munger. (2004). Post-field data quality control. In X. Lee, W. J. Massman & B. Law (Eds.), *Handbook of Micrometeorology: A guide for surface flux measurement and analysis* (pp. 181-208). Dordrecht: Kluwer Academic Publishers.
- García, Alfredo G., Di Bella, Carlos M., Houspanossian, Javier, Magliano, Patricio N., Jobbágy, Esteban G., Posse, Gabriela, . . . Noretto, Marcelo D. (2017). Patterns and controls of carbon dioxide and water vapor fluxes in a dry forest of central Argentina. *Agricultural and Forest Meteorology*, 247, 520-532. doi: <https://doi.org/10.1016/j.agrformet.2017.08.015>
- Gimenez, R, Noretto, M D, Mercu, J L, Paez, R, & Jobbágy, E G. (2016). The ecohydrological imprint of deforestation in the semi-arid Chaco: Insights from the last forest relicts of a highly cultivated landscape. *Hydrological Processes*, 30, 2603–2616.
- Glatzle, A. (2008). Gramíneas y leguminosas para el Chaco: adaptación, potencialidades. Asunción, Paraguay: INTTAS.
- Goward, Samuel N., & Dye, Dennis G. (1987). Evaluating North American net primary productivity with satellite observations. *Advances in Space Research*, 7(11), 165-174. doi: [https://doi.org/10.1016/0273-1177\(87\)90308-5](https://doi.org/10.1016/0273-1177(87)90308-5)
- Gowik, Udo, & Westhoff, Peter. (2011). The Path from C3 to C4 Photosynthesis. *Plant Physiology*, 155(1), 56. doi: 10.1104/pp.110.165308
- Hansen, M. C., Potapov, P. V., Moore, R., Hancher, M., Turubanova, S. A., Tyukavina, A., . . . Townshend, J. R. G. (2013). High-Resolution Global Maps of 21st-Century Forest Cover Change. *Science*, 342(6160), 850-853. doi: 10.1126/science.1244693
- Hastings, Steven J., Oechel, Walter C., & Muhlia-Melo, Arturo. (2005). Diurnal, seasonal and annual variation in the net ecosystem CO2 exchange of a desert shrub community (Sarcocaulis) in Baja California, Mexico. *Global Change Biology*, 11(6), 927-939. doi: 10.1111/j.1365-2486.2005.00951.x
- Hinojo-Hinojo, César, Castellanos, Alejandro E., Huxman, Travis, Rodriguez, Julio C., Vargas, Rodrigo, Romo-León, José R., & Biederman, Joel A. (2019). Native shrubland and managed buffelgrass savanna in drylands: Implications for ecosystem carbon and water fluxes. *Agricultural and Forest Meteorology*, 268, 269-278. doi: <https://doi.org/10.1016/j.agrformet.2019.01.030>
- Houspanossian, Javier, Giménez, Raúl, Baldi, Germán, & Noretto, Marcelo. (2016). Is aridity restricting deforestation and land uses in the South American Dry Chaco? *Journal of Land Use Science*, 11(4), 369-383. doi: 10.1080/1747423X.2015.1136707
- Houspanossian, Javier, Noretto, Marcelo, & Jobbágy, Esteban G. (2013). Radiation budget changes with dry forest clearing in temperate Argentina. *Global Change Biology*, 19, 1211-1222.
- Huntington, T G. (2006). Evidence for intensification of the global water cycle: review and synthesis. *Journal of Hydrology*, 319, 83-95.
- Huston, Michael A., & Wolverton, Steve. (2009). The global distribution of net primary production: resolving the paradox. *Ecological Monographs*, 79(3), 343-377. doi: doi:10.1890/08-0588.1
- Iriondo, M. (1993). Geomorphology and late quaternary of the Chaco (South America). *Geomorphology*, 7, 289-303.
- Jackson, R B, Canadell, J, Ehleringer, J R, Mooney, H A, Sala, O E, & Schulze, E D. (1996). A global analysis of root distributions for terrestrial biomes. *Oecologia*, 108, 389-411.
- Jackson, R B, Randerson, J T, Canadell, J, Anderson, R G, Avissar, R, Baldocchi, D D, . . . Pataki, D E. (2008). Protecting climate with forests. *Environmental Research Letters*, 3, doi:10.1088/1748-9326/1083/1084/044006.
- Jerry, R. Cox, Martin-R, M. H., Ibarra-F, F. A., Fourie, J. H., Rethman, J. F. G., & Wilcox, D. G. (1988). The Influence of Climate and Soils on the Distribution of Four African Grasses. *Journal of Range Management*, 41(2), 127-139. doi: 10.2307/3898948



- Jobbágy, E. G., Nosoetto, M. D., Villagra, P. E., & Jackson, R. B. (2011). Water subsidies from mountains to deserts: Their role in sustaining groundwater-fed oases in a sandy landscape. *Ecological Applications*, 21(3), 678-694.
- Jones, Hamlyn G. (1999). Use of infrared thermometry for estimation of stomatal conductance as a possible aid to irrigation scheduling. *Agricultural and Forest Meteorology*, 95(3), 139-149. doi: [https://doi.org/10.1016/S0168-1923\(99\)00030-1](https://doi.org/10.1016/S0168-1923(99)00030-1)
- Jones, Hamlyn G., Serraj, Rachid, Loveys, Brian R., Xiong, Lizhong, Wheaton, Ashley, & Price, Adam H. (2009). Thermal infrared imaging of crop canopies for the remote diagnosis and quantification of plant responses to water stress in the field. *Functional Plant Biology*, 36(11), 978-989. doi: <https://doi.org/10.1071/FP09123>
- Jung, Martin, Reichstein, Markus, Margolis, Hank A., Cescatti, Alessandro, Richardson, Andrew D., Arain, M. Altaf, . . . Williams, Christopher. (2011). Global patterns of land-atmosphere fluxes of carbon dioxide, latent heat, and sensible heat derived from eddy covariance, satellite, and meteorological observations. *Journal of Geophysical Research: Biogeosciences*, 116(G3). doi: 10.1029/2010jg001566
- Karlin, Marcos Sebastián, Karlin, Ulf Ola, Coirini, Rubén Omar, Reati, Gustavo Jorge, & Zapata, Ricardo Miguel. (2013). *El Chaco Árido*: Marcos Sebastián Karlin.
- Kunst, Carlos, Ledesma, Roxana, Bravo, Sandra, Albanesi, Ada, Anriquez, Analía, Van Meer, Howard, & Godoy, José. (2012). Disrupting woody steady states in the Chaco region (Argentina): responses to combined disturbance treatments. *Ecological Engineering*, 42, 42-53.
- Labraga, J. C., & Villalba, R. (2009). Climate in the Monte Desert: Past trends, present conditions, and future projections. *Journal of Arid Environments*, 73(2), 154-163. doi: <https://doi.org/10.1016/j.jaridenv.2008.03.016>
- Law, B. E., Falge, E., Gu, L., Baldocchi, D. D., Bakwin, P., Berbigier, P., . . . Wofsy, S. (2002). Environmental controls over carbon dioxide and water vapor exchange of terrestrial vegetation. *Agricultural and Forest Meteorology*, 113(1), 97-120. doi: [https://doi.org/10.1016/S0168-1923\(02\)00104-1](https://doi.org/10.1016/S0168-1923(02)00104-1)
- Li, Yuping, Li, Hongbin, Li, Yuanyuan, & Zhang, Suiqi. (2017). Improving water-use efficiency by decreasing stomatal conductance and transpiration rate to maintain higher ear photosynthetic rate in drought-resistant wheat. *The Crop Journal*, 5(3), 231-239. doi: <https://doi.org/10.1016/j.cj.2017.01.001>
- Liu, Fulai, Andersen, Mathias N., Jacobsen, Sven-Erik, & Jensen, Christian R. (2005). Stomatal control and water use efficiency of soybean (*Glycine max* L. Merr.) during progressive soil drying. *Environmental and Experimental Botany*, 54(1), 33-40. doi: <https://doi.org/10.1016/j.envexpbot.2004.05.002>
- Magliano, P N, Fernández, R J, Gimenez, R, Marchesini, V A, Páez, R A, & Jobbágy, E G. (2016). Cambios en la partición de flujos de agua en el Chaco Árido al reemplazar bosques por pasturas. *Ecología Austral*, 26, 95-106.
- Magliano, P N, Gimenez, R, Houspanossian, J, Páez, R, Nosoetto, M D, Fernández, R, & Jobbágy, E G. (2017a). Litter is more effective than forest canopy reducing soil evaporation in Dry Chaco rangelands. *Ecohydrology*, e1879. <https://doi.org/10.1002/eco.1879>.
- Magliano, P N, Mindham, D, Tych, W, Murray, F, Nosoetto, M D, Jobbágy, E G, . . . Chappell, N A. (2019a). Hydrological functioning of cattle ranching impoundments in the Dry Chaco rangelands of Argentina. *Hydrology Research*, 50(6), 1596-1608. doi: 10.2166/nh.2019.149
- Magliano, P N, Whitworth-Hulse, J I, & Baldi, G. (2019b). Interception, throughfall and stemflow partition in drylands: Global synthesis and meta-analysis. *Journal of Hydrology*, 568, 638-645. doi: <https://doi.org/10.1016/j.jhydrol.2018.10.042>
- Magliano, P N, Whitworth-Hulse, J I, Florio, E L, Aguirre, E C, & Blanco, L J. (2019c). Interception loss, throughfall and stemflow by *Larrea divaricata*: The role of rainfall characteristics and plant morphological attributes. *Ecological Research*, 34(6), 753-764. doi: 10.1111/1440-1703.12036
- Magliano, P. N., Breshears, D. D., Fernández, R. J., & Jobbágy, E. G. (2015). Rainfall intensity switches ecohydrological runoff/runon redistribution patterns in dryland vegetation patches. *Ecological Applications*, 25(8), 2094-2100. doi: 10.1890/15-0550.1

- Magliano, P. N., Fernández, R. J., Florio, E. L., Murray, F., & Jobbágy, E.G. (2017b). Soil physical changes after conversion of woodlands to pastures in Dry Chaco rangelands (Argentina). *Rangeland Ecology & Management*, *70*, 225-229.
- Marchesini, V A, Fernández, R J, & Jobbágy, E G. (2013). Salt leaching leads to drier soils in disturbed semiarid woodlands of central Argentina. *Oecologia*, *171*(4), 1003-1012. doi: 10.1007/s00442-012-2457-y
- Marchesini, V A, Gimenez, R, Nosetto, M D, & Jobbágy, E G. (2016). The ecohydrological transformation of Chaco Dry Forests and the risk of dryland salinity: are we following Australia's footsteps? *Ecohydrology*, *e1822*. doi: 10.1002/eco.1822.
- Marshall, V. M., Lewis, M. M., & Ostendorf, B. (2012). Buffel grass (*Cenchrus ciliaris*) as an invader and threat to biodiversity in arid environments: A review. *Journal of Arid Environments*, *78*, 1-12. doi: <https://doi.org/10.1016/j.jaridenv.2011.11.005>
- Milkovic, Mayra, Paruelo, José M., & Nosetto, Marcelo D. (2019). Hydrological impacts of afforestation in the semiarid Patagonia: A modelling approach. *Ecohydrology*, *0*(0), e2113. doi: 10.1002/eco.2113
- Myneni, R B, & Park, T. (2015). MCD15A2H MODIS/Terra+Aqua Leaf Area Index/FPAR 8-day L4 Global 500m SIN Grid V006. NASA EOSDIS Land Processes DAAC. <https://doi.org/10.5067/MODIS/MCD15A2H.006>.
- Namur, Pedro, Tessi, J M, Avila, R E, Rettore, H A, & Ferrando, C A. (2014). *Buffel Grass. Generalidades, implantación y manejo para recuperación de áreas degradadas*. Córdoba, Argentina: INTA.
- New, M, Lister, D, Hulme, M, & Makin, I. (2002). A high-resolution data set of surface climate over global land areas. *Climate Research*, *21*, 1-25.
- Newman, B P, Archer, S, Breshears, D D, Dahm, C, Duffy, C J, McDowell, N G, . . . Vivoni, E R. (2006). Ecohydrology of water-limited environments: A scientific vision. *Water Resources Research*, *42*, W06302, doi:06310.01029/02005WR004141.
- Nosetto, M D, Jobbágy, E G, Brizuela, A B, & Jackson, R B. (2012). The hydrologic consequences of land cover change in central Argentina. *Agriculture, Ecosystems and Environment*, *154*, 2-11.
- Paruelo, J.M., Guerschman, J.P., Baldi, G., & Di Bella, C.M. (2004). La estimación de la superficie agrícola. Antecedentes y una propuesta metodológica. *Interciencia*, *29*, 421-427.
- Pastorello, Gilberto, Trotta, Carlo, Canfora, Eleonora, Chu, Housen, Christianson, Danielle, Cheah, You-Wei, . . . Papale, Dario. (2020). The FLUXNET2015 dataset and the ONEFlux processing pipeline for eddy covariance data. *Scientific Data*, *7*(1), 225. doi: 10.1038/s41597-020-0534-3
- Peña Zubiate, C A, Anderson, D L, Demmi, M A, Saenz, J L, & D'Hiriart, A (Eds.). (1998). *Carta de suelos y vegetación de la provincia de San Luis*. San Luis, Argentina: Instituto Nacional de Tecnología Agropecuaria (INTA).
- Posse, Gabriela, Richter, Klaus, Lewczuk, Nuria, Cristiano, Piedad, Gattinoni, Natalia, Rebella, César, & Achkar, Antonio. (2014). Attribution of Carbon Dioxide Fluxes to Crop Types in a Heterogeneous Agricultural Landscape of Argentina. *Environmental Modeling & Assessment*, *19*(5), 361-372. doi: 10.1007/s10666-013-9395-x
- Poulter, Benjamin, Frank, David, Ciais, Philippe, Myneni, Ranga B., Andela, Niels, Bi, Jian, . . . van der Werf, Guido R. (2014). Contribution of semi-arid ecosystems to interannual variability of the global carbon cycle. *Nature*, *509*(7502), 600-603. doi: 10.1038/nature13376
- Právělie, Remus. (2016). Drylands extent and environmental issues. A global approach. *Earth-Science Reviews*, *161*, 259-278. doi: <https://doi.org/10.1016/j.earscirev.2016.08.003>
- Reichstein, Markus, Falge, Eva, Baldocchi, Dennis, Papale, Dario, Aubinet, Marc, Berbigier, Paul, . . . Valentini, Riccardo. (2005). On the separation of net ecosystem exchange into assimilation and ecosystem respiration: review and improved algorithm. *Global Change Biology*, *11*(9), 1424-1439. doi: 10.1111/j.1365-2486.2005.001002.x
- Reichstein, Markus, Tenhunen, John D., Rouspard, Olivier, Ourcival, Jean-marc, Rambal, Serge, Miglietta, Franco, . . . Valentini, Riccardo. (2002). Severe drought effects on ecosystem CO2 and H2O fluxes at three Mediterranean evergreen sites: revision of current hypotheses? *Global Change Biology*, *8*(10), 999-1017. doi: 10.1046/j.1365-2486.2002.00530.x

- Reynolds, J. F., Stafford Smith, D. M., Lambin, E. F., Turner II, B. L., Mortimore, M., Batterbury, S. P. J., . . . Walker, B. (2007). Ecology: Global desertification: Building a science for dryland development. *Science*, *316*(5826), 847-851. doi: 10.1126/science.1131634
- Reynolds, James F, Kemp, Paul R, Ogle, Kiona, & Fernández, Roberto J. (2004). Modifying the 'pulse-reserve' paradigm for deserts of North America: precipitation pulses, soil water, and plant responses. *Oecologia*, *141*(2), 194-210.
- Rotenberg, E, & Yakir, D. (2010). Contribution of Semi-Arid Forests to the Climate System. *Science*, *327*, 451-454.
- Rueda, Carla V., Baldi, Germán, Gasparri, Ignacio, & Jobbágy, Esteban G. (2015). Charcoal production in the Argentine Dry Chaco: Where, how and who? *Energy for Sustainable Development*, *27*, 46-53. doi: <https://doi.org/10.1016/j.esd.2015.04.006>
- Sage, Rowan F., & Zhu, Xin-Guang. (2011). Exploiting the engine of C4 photosynthesis. *Journal of Experimental Botany*, *62*(9), 2989-3000. doi: 10.1093/jxb/err179
- Santoni, C S, Jobbágy, E G, & Contreras, S. (2010). Vadose transport of water and chloride in dry forests of central Argentina: the role of land use and soil texture. *Water Resources Research*, *46*(10), W10541. doi: 10.1029/2009WR008784
- Scott, R L, Jenerette, G D, Potts, D L, & Huxman, T E. (2009). Effects of seasonal drought on net carbon dioxide exchange from a woody-plant-encroached semiarid grassland. *Journal of Geophysical Research*, *114*, G04004, doi:04010.01029/02008JG000900.
- Scott, Russell L., Biederman, Joel A., Hamerlynck, Erik P., & Barron-Gafford, Greg A. (2015). The carbon balance pivot point of southwestern U.S. semiarid ecosystems: Insights from the 21st century drought. *Journal of Geophysical Research: Biogeosciences*, *120*(12), 2612-2624. doi: 10.1002/2015jg003181
- Schimel, David S. (2010). Drylands in the earth system. *Science*, *327*(5964), 418-419.
- Schwalm, Christopher, Williams, Christopher, Schaefer, Kevin, Arneth, Almut, Bonal, Damien, Buchmann, Nina, . . . Richardson, Andrew. (2010). Assimilation exceeds respiration sensitivity to drought: A FLUXNET synthesis. *Global Change Biology*, *16*(2), 657-670. doi: doi:10.1111/j.1365-2486.2009.01991.x
- Seyfried, Mark S., & Wilcox, Bradford P. (2006). Soil water storage and rooting depth: key factors controlling recharge on rangelands. *Hydrological Processes*, *20*(15), 3261-3275. doi: 10.1002/hyp.6331
- Silva, Paulo Ferreira da, Lima, José Romualdo de Sousa, Antonino, Antonio Celso Dantas, Souza, Rodolfo, Souza, Eduardo Soares de, Silva, José Raliuson Inácio, & Alves, Edevaldo Miguel. (2017). Seasonal patterns of carbon dioxide, water and energy fluxes over the Caatinga and grassland in the semi-arid region of Brazil. *Journal of Arid Environments*, *147*, 71-82. doi: <https://doi.org/10.1016/j.jaridenv.2017.09.003>
- Sims, D A, Rahman, A, Cordova, V D, El-Masri, B Z, Baldocchi, D D, Flanagan, L B, . . . Xu, L. (2006). On the use of MODIS EVI to assess gross primary productivity of North American ecosystems. *Journal of Geophysical Research*, *111*, G4, G04015 04010.01029/02006JG000162.
- Steinaker, Diego F., Jobbágy, Esteban G., Martini, Juan P., Arroyo, Daniel N., Pacheco, Jorge L., & Marchesini, Victoria A. (2016). Vegetation composition and structure changes following roller-chopping deforestation in central Argentina woodlands. *Journal of Arid Environments*, *133*, 19-24. doi: <http://dx.doi.org/10.1016/j.jaridenv.2016.05.005>
- Trenberth, K. E., Jones, P D, Ambenje, P, Bojariu, R, Easterling, D R, Klein Tank, A M G, . . . Zhai, P. (2007). Observations: surface and atmospheric climate change. In S. D. Salomon, D. Qin, M. Manning, Z. Chien, M. Marquis, K. B. Averyt, M. Tignor & H. L. Miller (Eds.), *Climate Change 2007: The Physical Science Basis. Contribution of Working Group I to the Fourth Assessment Report of the Intergovernmental Panel on Climate Change* (pp. 235-336). Cambridge, UK.: Cambridge University Press.
- Wang, L, d'Odorico, P, Evans, JP, Eldridge, DJ, McCabe, MF, Caylor, KK, & King, EG. (2012). Dryland ecohydrology and climate change: critical issues and technical advances. *Hydrology and Earth System Sciences*, *16*(8), 2585-2603.

- Webb, E. K., Pearman, G. I., & Leuning, R. (1980). Correction of flux measurements for density effects due to heat and water vapour transfer. *Quarterly Journal of the Royal Meteorological Society*, 106(447), 85-100. doi: 10.1002/qj.49710644707
- Wilczak, James M., Oncley, Steven P., & Stage, Steven A. (2001). Sonic Anemometer Tilt Correction Algorithms. *Boundary-Layer Meteorology*, 99(1), 127-150. doi: 10.1023/a:1018966204465
- Wilson, K B, Goldstein, A, Falge, E, Aubinet, A, Baldocchi, D, Berbigier, P, . . . Verma, Shashi. (2002). Energy balance closure at FLUXNET sites. *Agricultural and Forest Meteorology*, 113, 223-243.
- Wohlfahrt, Georg, Fenstermaker, L, & Arnone III, J A. (2008). Large annual net ecosystem CO<sub>2</sub> uptake of a Mojave Desert ecosystem. *Global Change Biology*, 14(7), 1475-1487. doi: 10.1111/j.1365-2486.2008.01593.x
- Xu, Hao-jie, Wang, Xin-ping, Zhao, Chuan-yan, & Zhang, Xiao-xiao. (2019). Responses of ecosystem water use efficiency to meteorological drought under different biomes and drought magnitudes in northern China. *Agricultural and Forest Meteorology*, 278, 107660. doi: https://doi.org/10.1016/j.agrformet.2019.107660
- Yang, Yuting, Guan, Huade, Batelaan, Okke, McVicar, Tim R., Long, Di, Piao, Shilong, . . . Simmons, Craig T. (2016). Contrasting responses of water use efficiency to drought across global terrestrial ecosystems. *Scientific Reports*, 6, 23284.
- Yi, Chuixiang, Ricciuto, Daniel, Li, Runze, Wolbeck, John, Xu, Xiyan, Nilsson, Mats, . . . Zhao, Xinquan. (2010). Climate control of terrestrial carbon exchange across biomes and continents. *Environmental Research Letters*, 5(3), 034007. doi: 10.1088/1748-9326/5/3/034007
- Zeng, Ning, Qian, Haifeng, Munoz, Ernesto, & Iacono, Roberto. (2004). How strong is carbon cycle-climate feedback under global warming? *Geophysical Research Letters*, 31(20). doi: doi:10.1029/2004GL020904
- Zhang, Jinqing, Jiang, Hong, Song, Xinzhang, Jin, Jiabin, & Zhang, Xiuying. (2018). The Responses of Plant Leaf CO<sub>2</sub>/H<sub>2</sub>O Exchange and Water Use Efficiency to Drought: A Meta-Analysis. *Sustainability*, 10(2), 551.
- Zuzek, Andres B. (1978). *Descripción geológica de la Hoja 18f, Chamental, Provincia de La Rioja: carta geológico-económica de la República Argentina, escala 1: 200.000*: Servicio Geológico Nacional.